Leveraging Spectroscopy for Photometric Survey Science

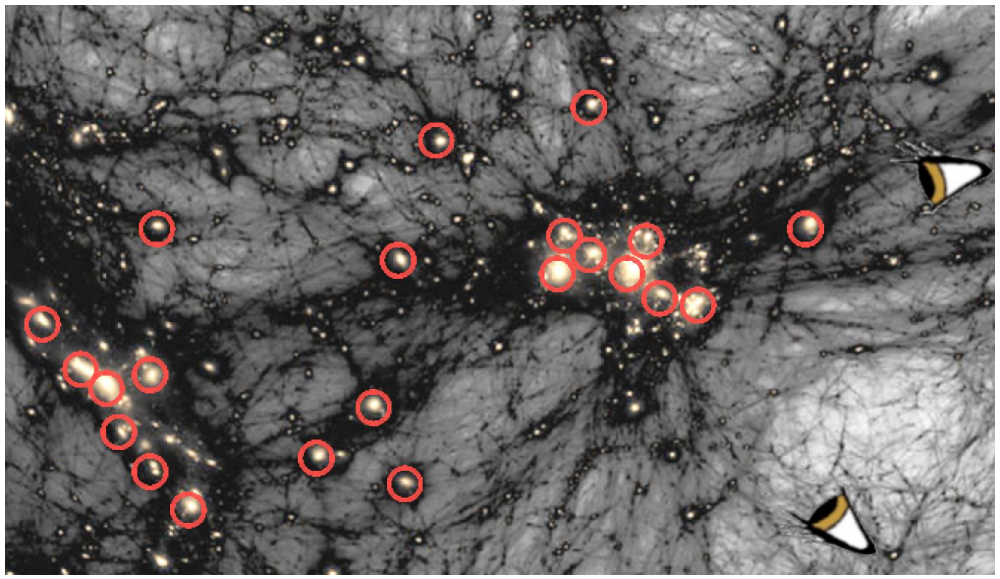

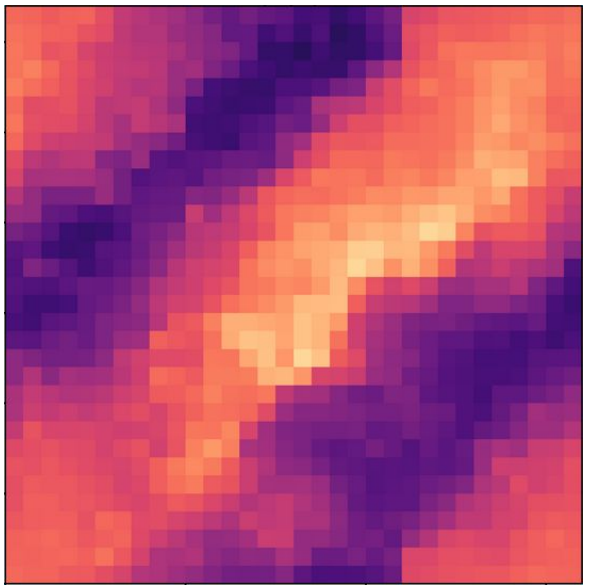

Justin Myles

Advised by: Steve Allen, Alex Amon, Daniel Gruen, Adam Mantz

Work done with the tireless support of many collaborators in the Dark Energy Survey

I. Motivation

II. Quantifying Projection Effects in redMaPPer Clusters

III. DES Year 3 Weak Lensing Source Galaxy Redshift Calibration

Cosmic shear is host to a debate about redshifts.

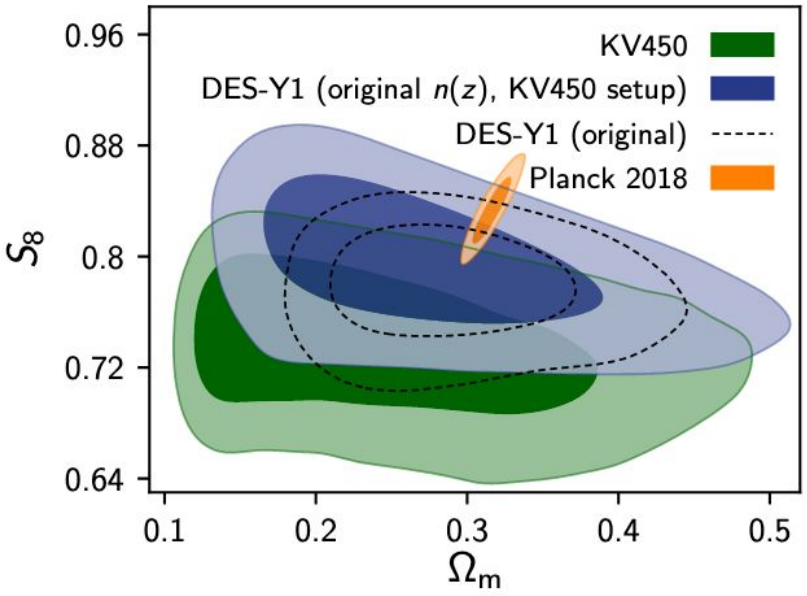

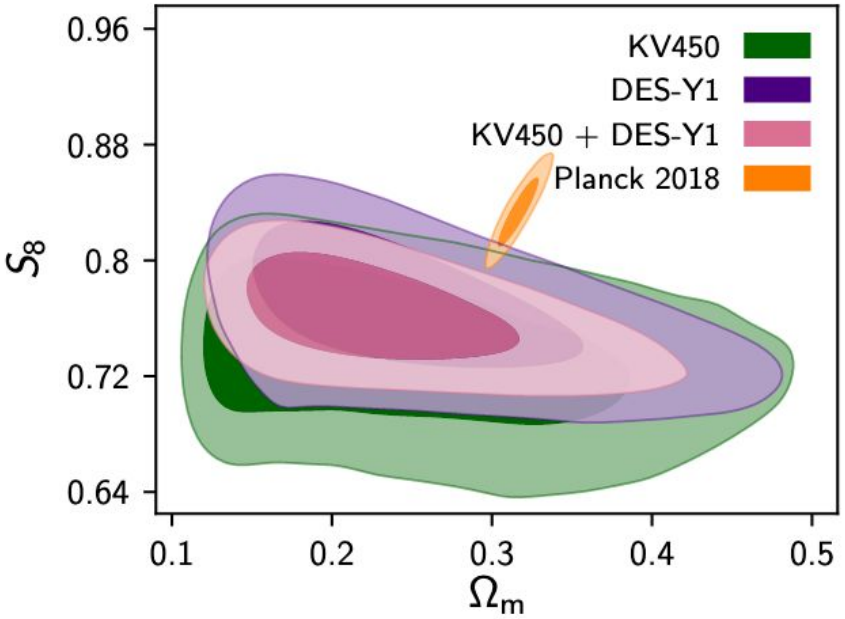

Joudaki et al. 2019

Optical cluster cosmology is host to a mysterious result.

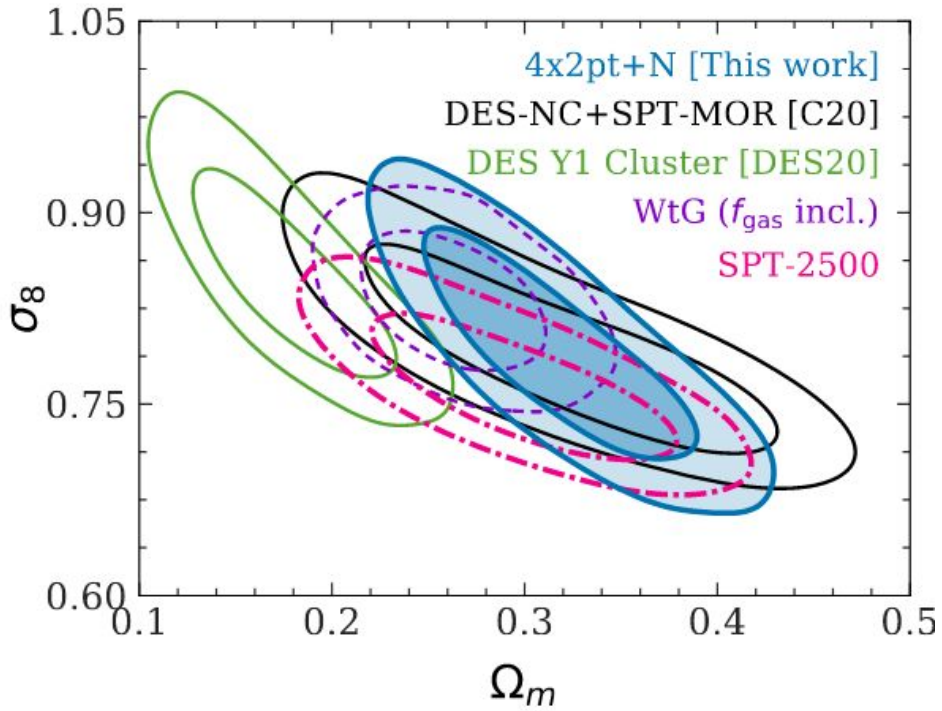

DES Collaboration et al. 2020; To et al. 2020

The Dark Energy Survey is among a group of leading cosmology experiments.

- 4m Blanco Telescope
- ~5000 square degree wide field survey in *g r i z Y* over 6 years
- >100M Y3 Galaxy Source Catalog
- 27 square degree deep time-domain survey in *u g r i z Y* overlapping with archival *Y J H K*
  - 8 square degree *ugrizJHK* used for DES Y3

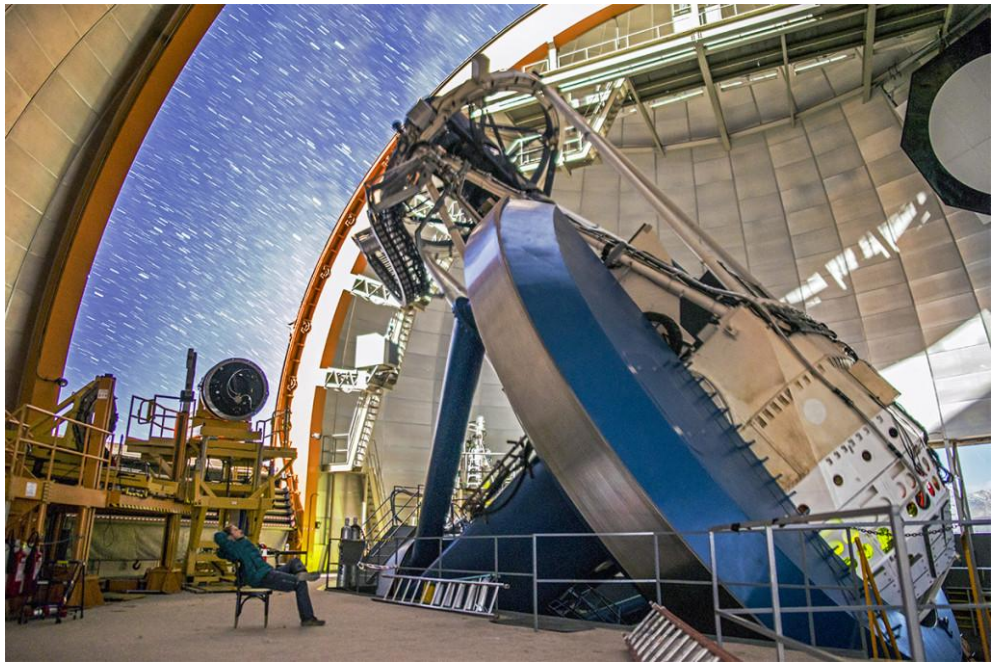

I. Motivation

II. Quantifying Projection Effects in redMaPPer Clusters

III. DES Year 3 Weak Lensing Source Galaxy Redshift Calibration

The cluster mass function is sensitive to the parameters of the cosmological model for the Universe, but relating cluster mass to observables is fraught with challenges.

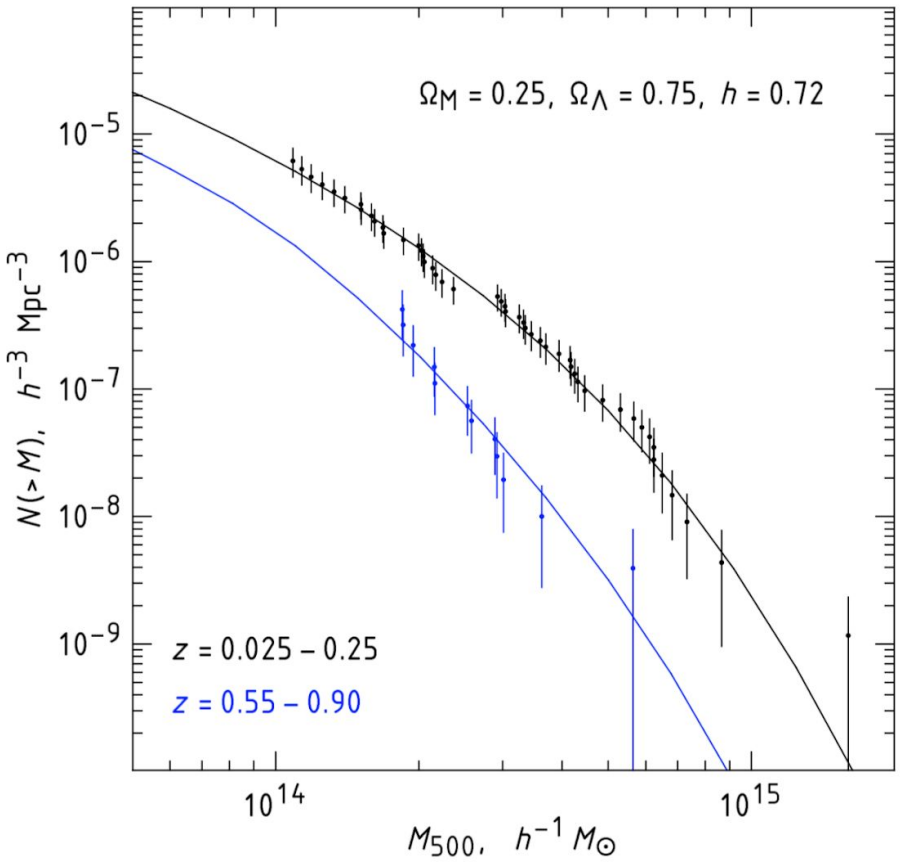

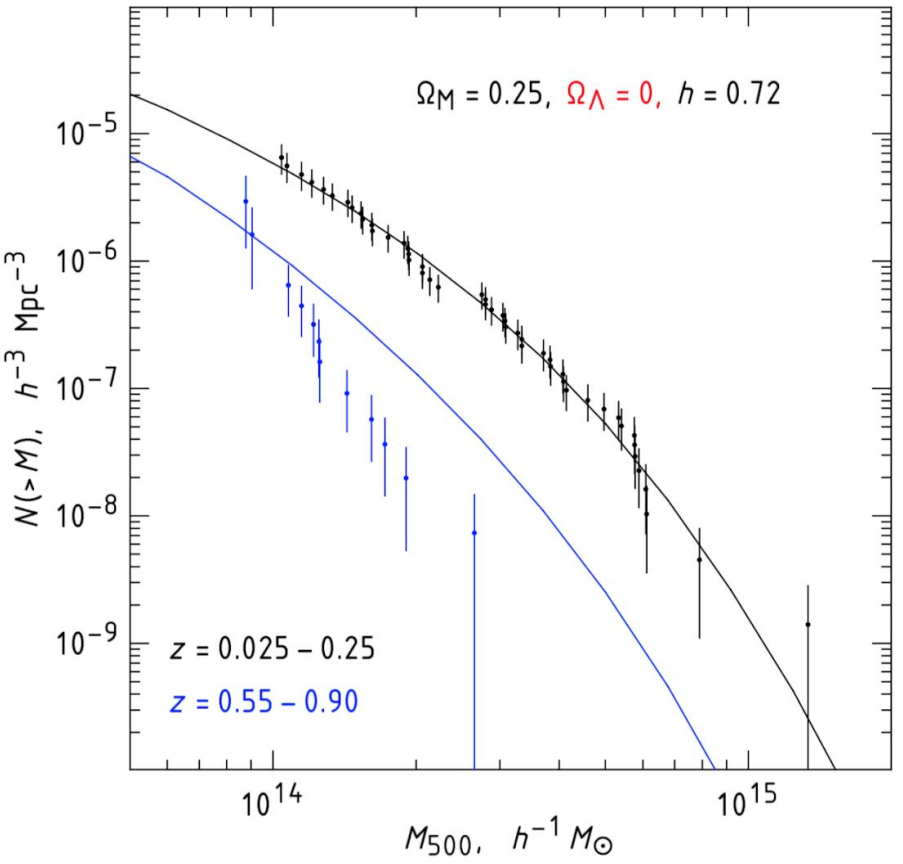

Vikhlinin et al. 2009b

Optical cluster cosmology relies on cluster richness as a proxy for mass.

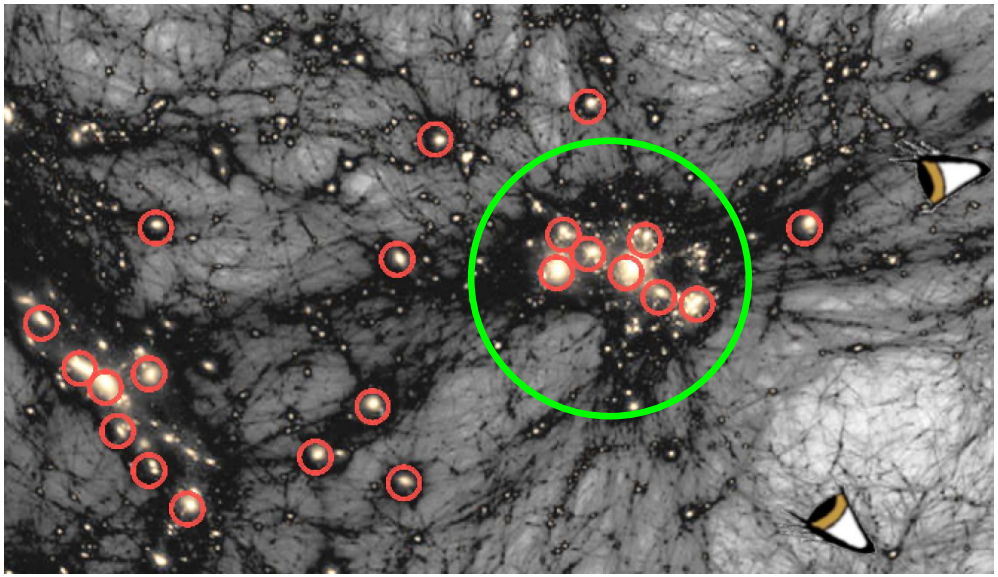

Dark Sky Simulations / Ralf Kaehler, Carter Emmart, Tom Abel, Oliver Hahn / SLAC

Can spectroscopy help empirically calibrate the projection effects model?

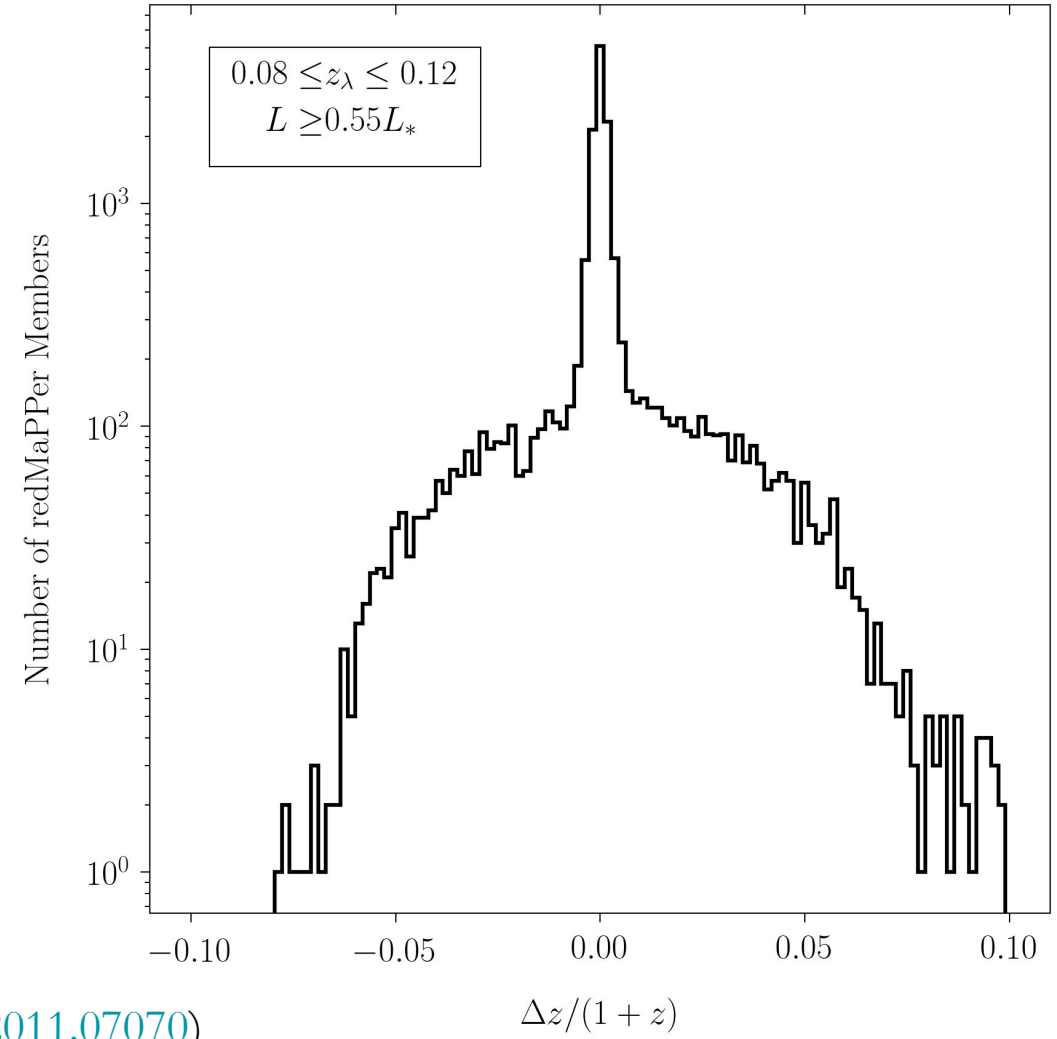

Myles et al. 2020 (arXiv: 2011.07070)

Projection effects can be quantified using a simple two Gaussian model.

$$p(\Delta z/(1+z)) = f_{\rm cl}\,\mathcal{N}(\Delta z/(1+z)\,|\mu_{\rm cl},\sigma_{\rm cl}) + f_{\rm proj}\,\mathcal{N}(\Delta z/(1+z)\,|\mu_{\rm proj},\sigma_{\rm proj}),$$

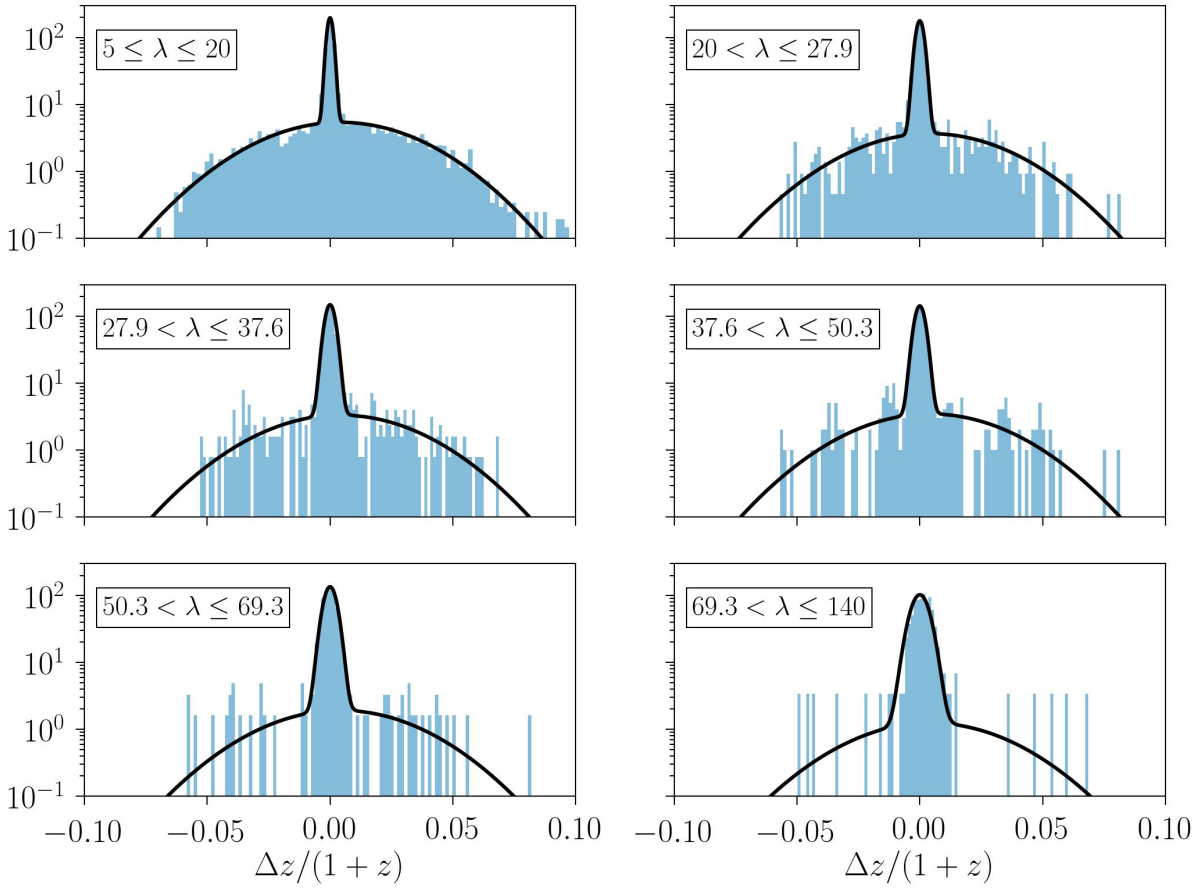

Myles et al. 2020 (arXiv: 2011.07070)

Projection effects are a strong function of richness.

$$b_{\lambda,j} \equiv \frac{\sum \lambda^{L \geq 0.55\, L_\star} - \sum \lambda_{\rm spec}{}^{L \geq 0.55\, L_\star}}{\sum \lambda^{L \geq 0.55\, L_\star}}.$$

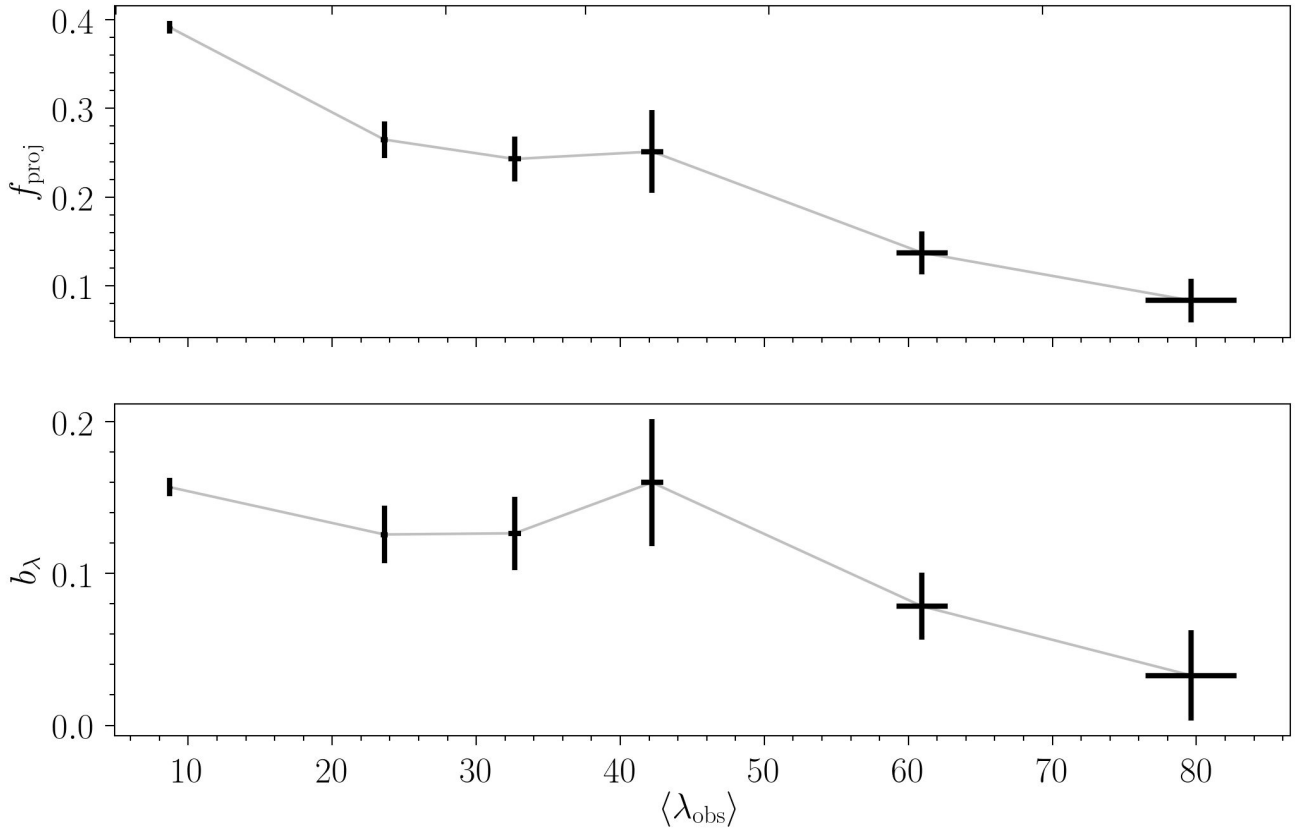

Myles et al. 2020 (arXiv: 2011.07070)

Our measurement has a steeper richness dependence than recent models.

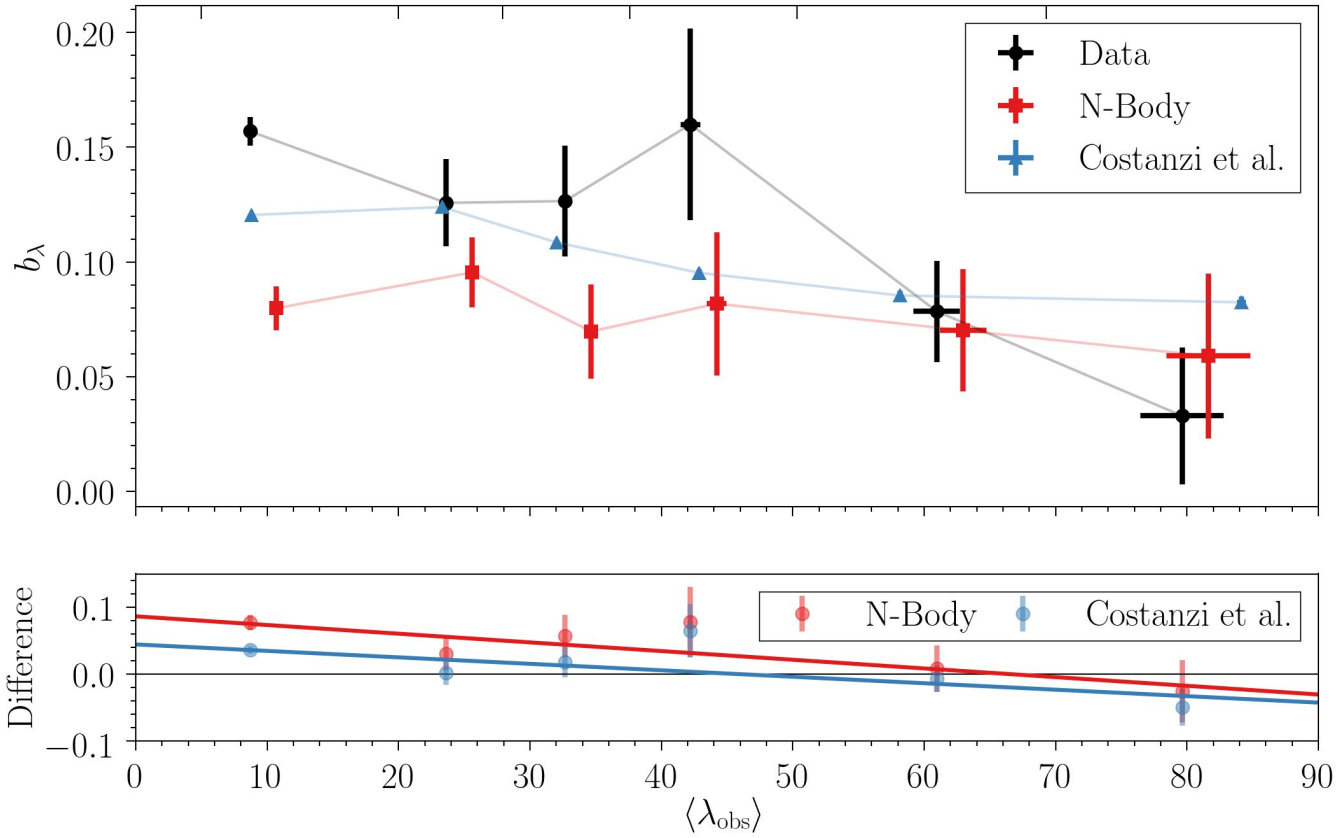

Myles et al. 2020 (arXiv: 2011.07070)

Velocity dispersion scales with spectroscopically calibrated richness in a way consistent with self-similarity.

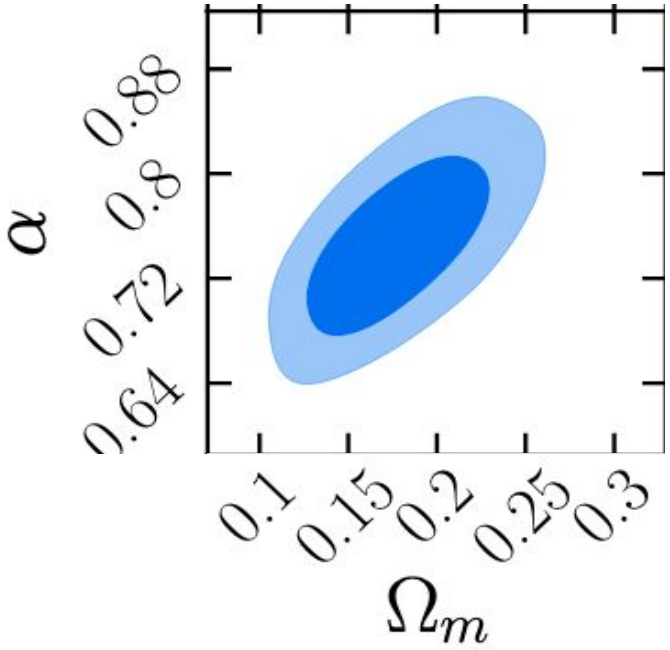

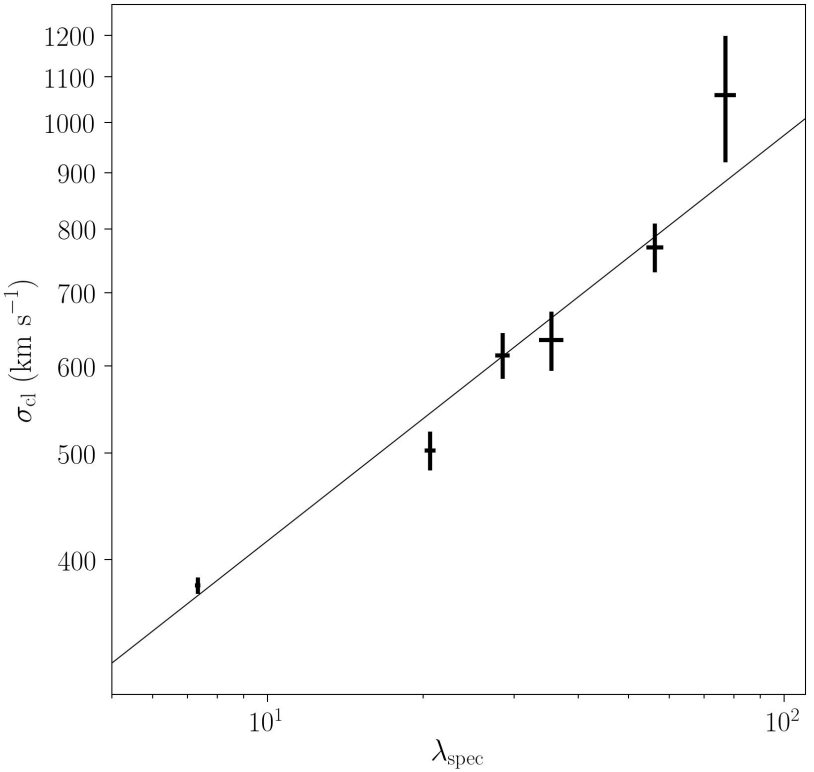

DES Collaboration et al. 2020; Myles et al. 2020 (arXiv: 2011.07070)

Projection effects are not a strong function of galaxy luminosity.

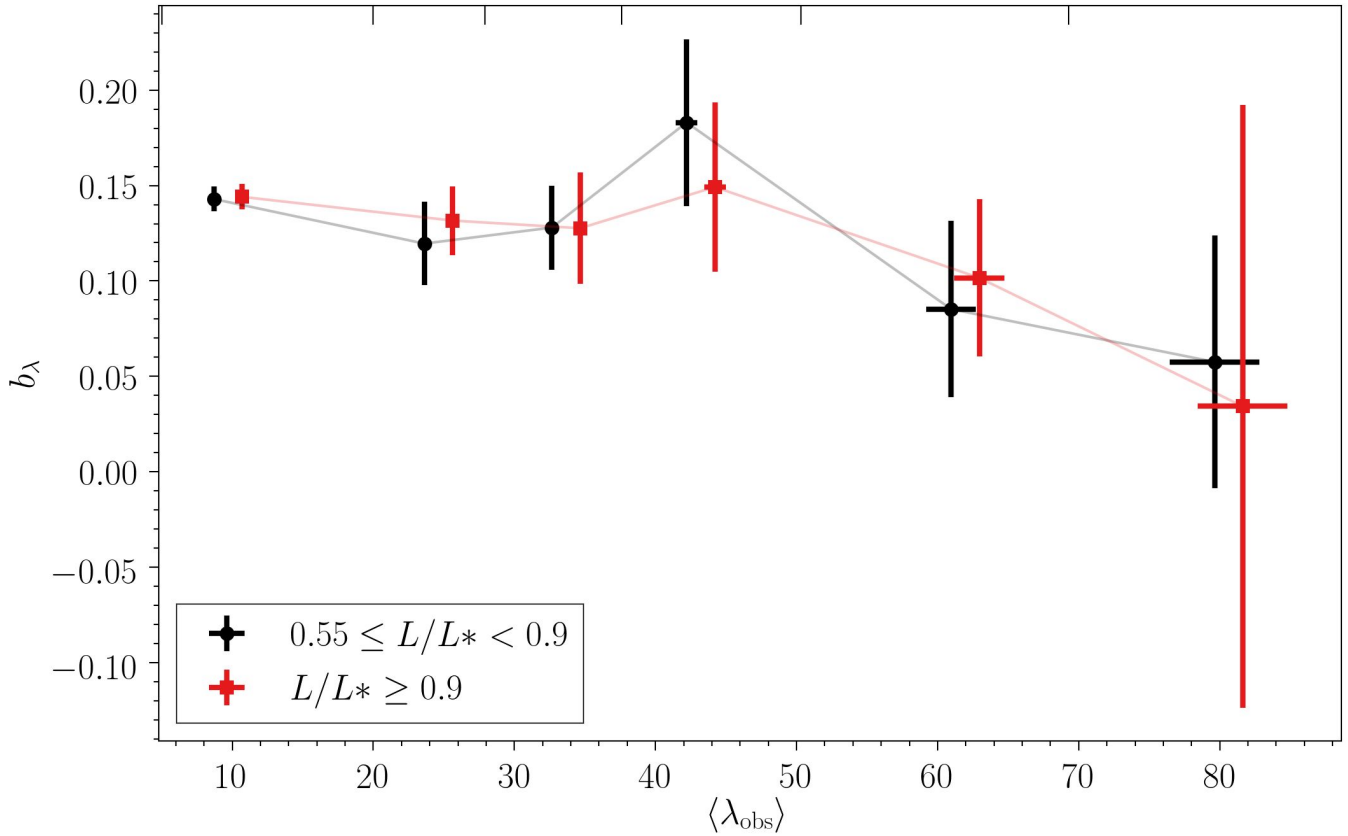

Myles et al. 2020 (arXiv: 2011.07070)

Observing Effort for DES Y3

Goal: multi-purpose sample of richness-redshift selected representative redMaPPer member spectra by end of year

Redshift	Richness	Telescope/Instrument (P.I.)	Status
~0.1 (SDSS)	>5	SDSS Legacy Program, SDSS Special Program, SEGUE-1, SEGUE-2	Completed
~0.1 (SDSS)	30	WIYN/Hydra (Myles)	Observed
<0.2 (SDSS)	>5	DESI Bright Galaxy Sample	
<0.2 (SDSS)	>20	DESI Spare Fiber Proposal (Golden-Marx)	Pending
~0.45	30	Gemini/GMOS (Gruen; Baxter)	Observed
~0.45	>60	Magellan/M2FS (Chang; Miller; Rozo)	Observed
~0.45	30	Keck/LRIS (Baxter; Jeltema)	Observed
~0.7	30	Keck/LRIS (Baxter, Jeltema)	Observed

I. Motivation

II. Quantifying Projection Effects in redMaPPer Clusters

III. DES Year 3 Weak Lensing Source Galaxy Redshift Calibration

A. 3x2pt. cosmology with the Dark Energy Survey

B. SOMPZ: a novel method for weak lensing redshift calibration

C. DES Y3 Results

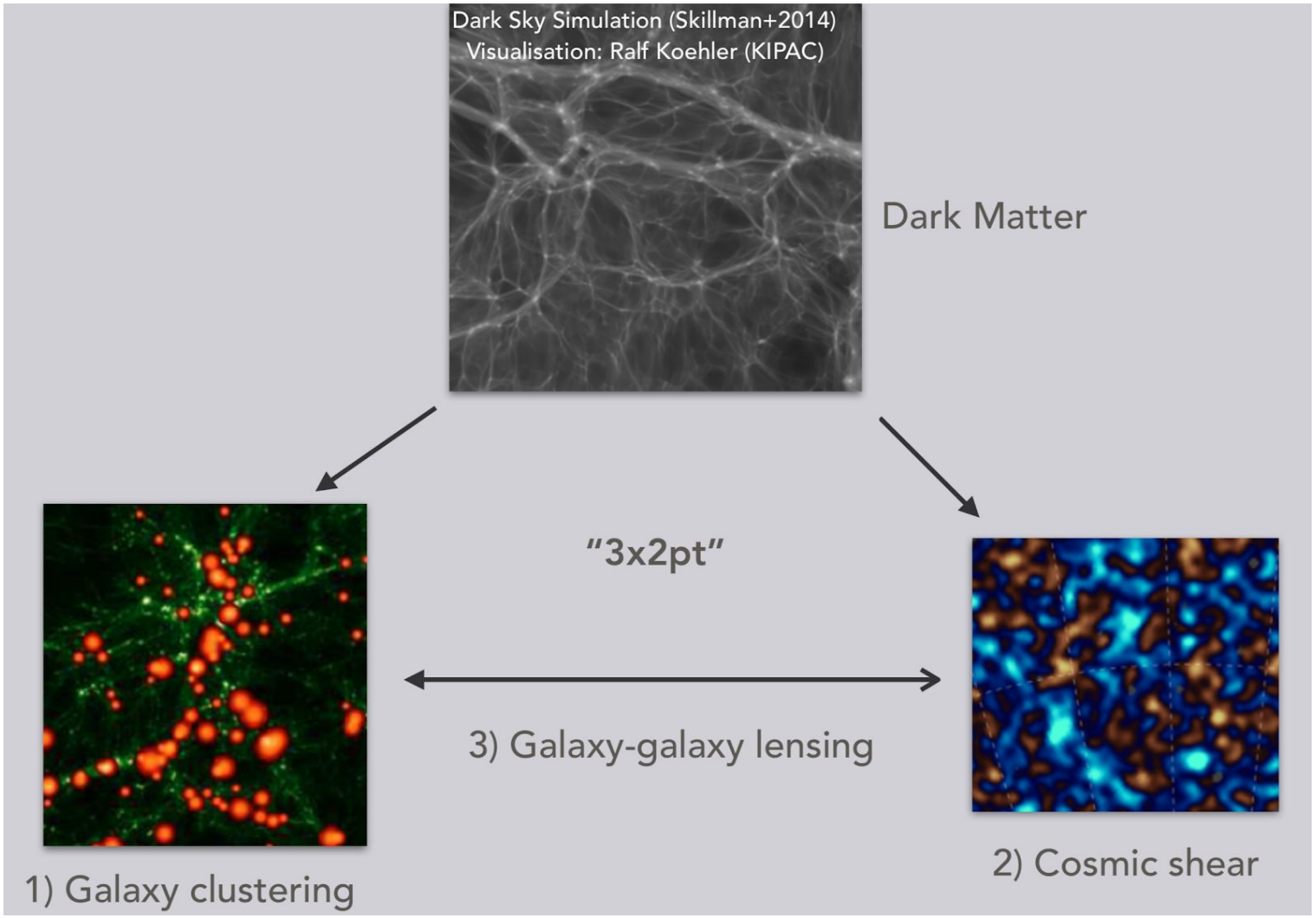

Slide credit:
Daniel Gruen, Niall MacCrann, Michael Troxel

Testing a cosmological model with cosmic shear depends on a statistical ensemble of two basic measurements: galaxy shapes and redshifts.

$$P_\kappa^{ij}(\ell) = \int_0^{\chi_H} d\chi \frac{q^i(\chi) q^j(\chi)}{\chi^2} P_{\rm NL}\left(\frac{\ell + 1/2}{\chi}, \chi\right)$$

$$\hat{\xi}_\pm^{ij}(\theta) = \frac{1}{2\pi} \int d\ell \ell J_{0/4}(\theta\ell) P_\kappa^{ij}(\ell)$$

$$q^i(\chi) = \frac{3}{2}\Omega_m \left(\frac{H_0}{c}\right)^2 \frac{\chi}{a(\chi)} \int_\chi^{\chi_H} d\chi' n^i(\chi') \frac{\chi' - \chi}{\chi'}$$

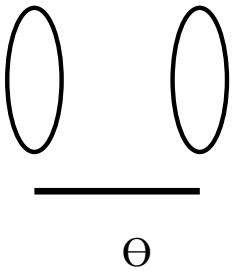

Θ

The similar alignment of these two galaxies leads to a positive contribution to ξ^+

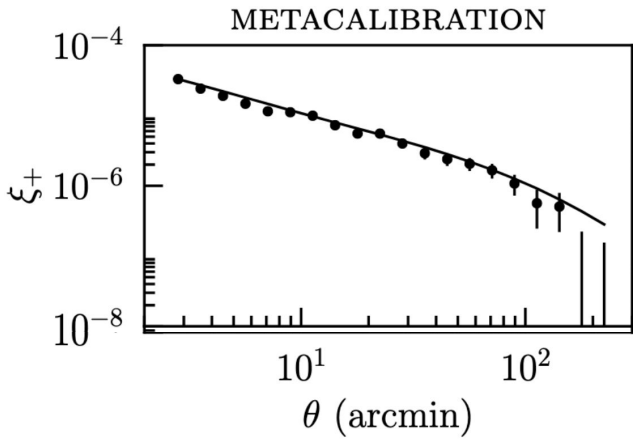

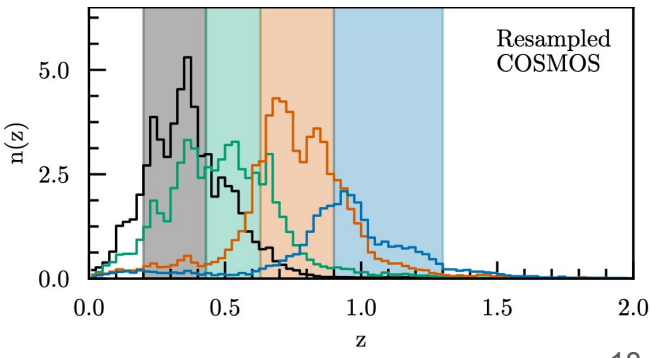

Troxel et al. 2018

Neither of the two prevailing photo-z solution paradigms solve the real problem: degeneracies in the statistical color-redshift relation.

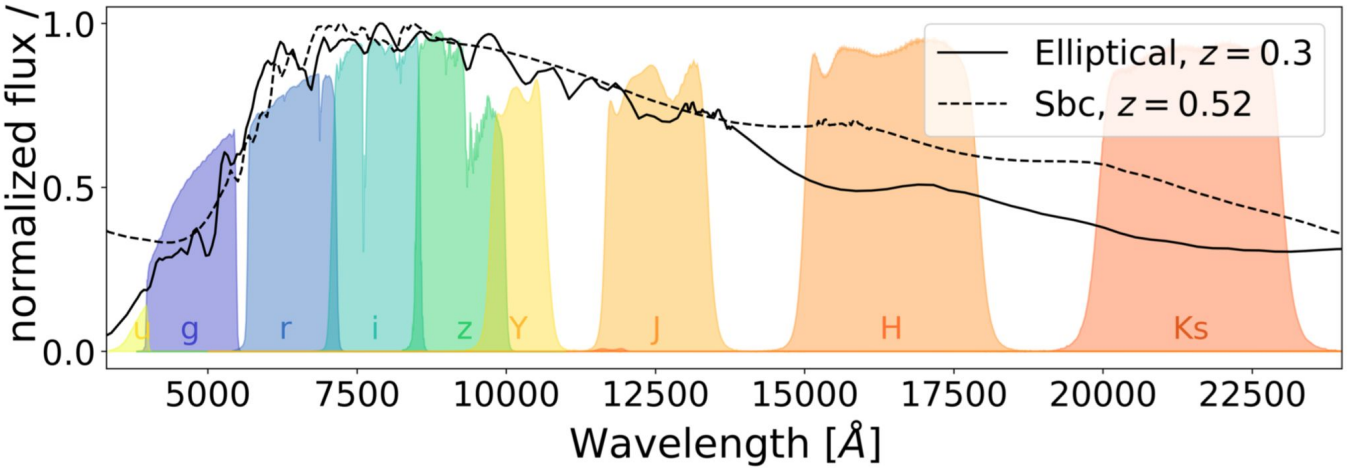

1. Machine learning models trained with biased or incomplete spectroscopic samples.
2. Template fitting codes rely on analytical recipes that can be insufficient to describe the observed color-redshift relation.

Buchs & Davis et al. 2019

Selection biases introduced by using spectroscopic redshift samples are key to the redshift debate.

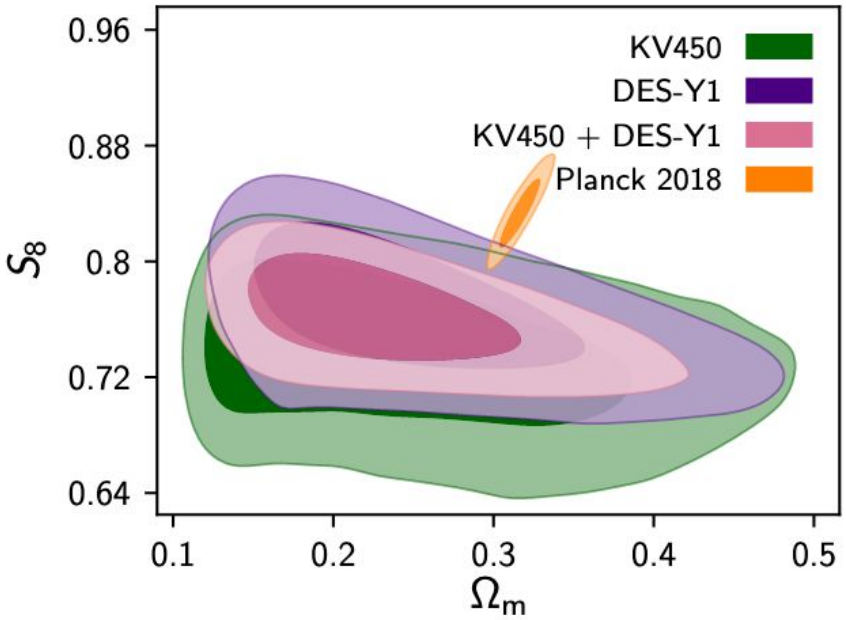

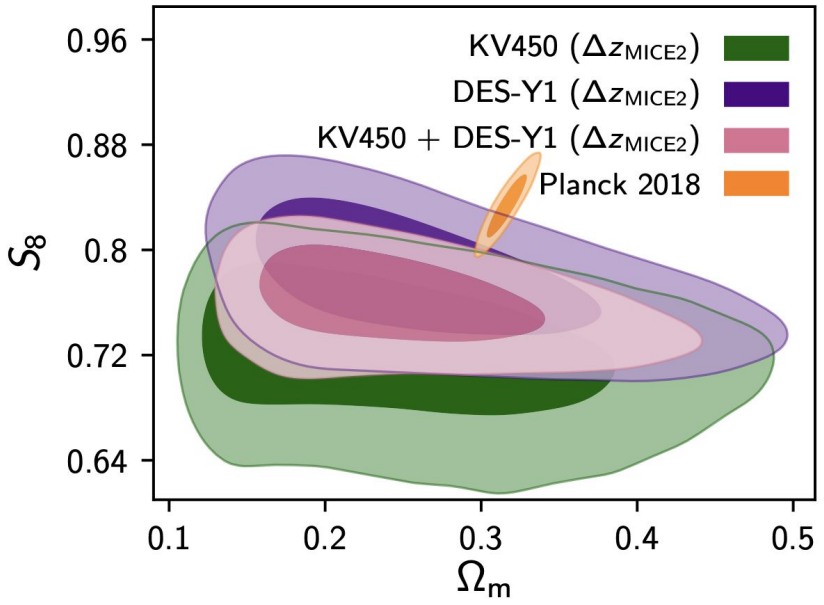

Joudaki et al. 2019

I. Motivation

II. Quantifying Projection Effects in redMaPPer Clusters

III. DES Year 3 Weak Lensing Source Galaxy Redshift Calibration

A. 3x2pt. cosmology with the Dark Energy Survey

B. SOMPZ: a novel method for weak lensing redshift calibration

C. DES Y3 Results

SOMPZ is one part of a larger DES Y3 redshift effort. Our work focuses on how to leverage the deep fields to break the key degeneracies in the statistical color-redshift relation.

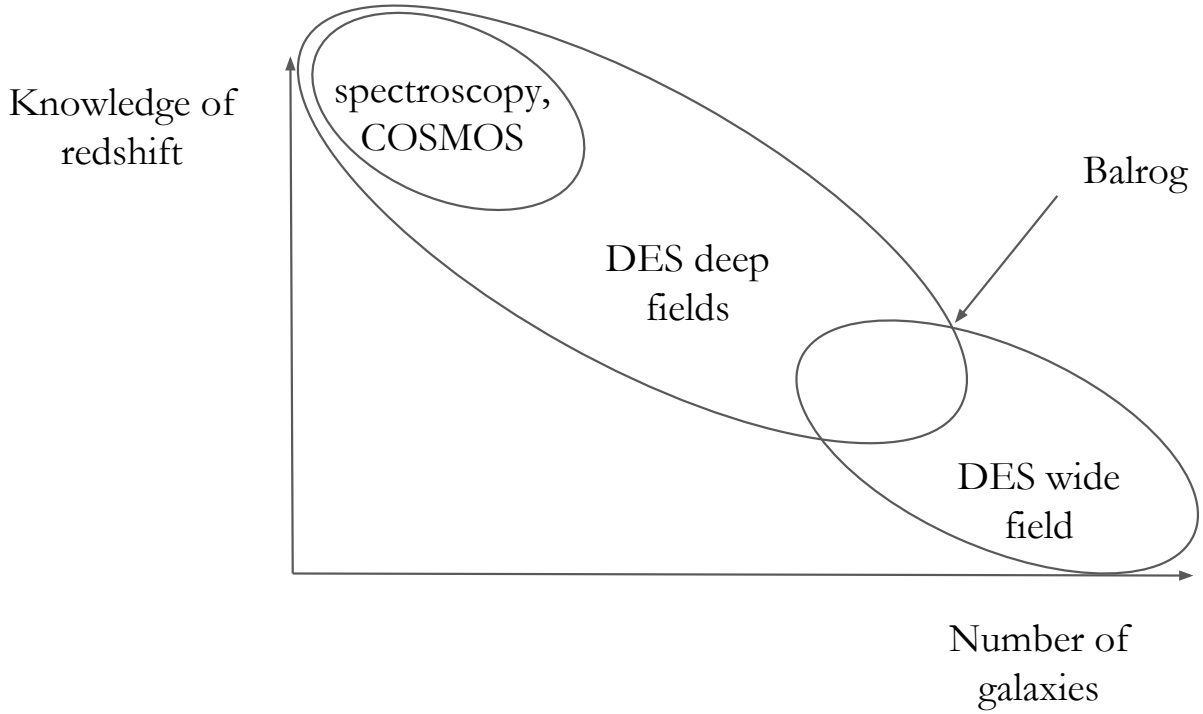

Leveraging the deep fields to improve our knowledge of the statistical color-redshift relation amounts to marginalizing over deep photometric information.

$$p(z|r,i,z) = \int p(z|u,g,r,i,z,J,H,K)\,p(u,g,r,i,z,J,H,K|r,i,z)\,d[u,g,r,i,z,J,H,K]$$

p(z) at a given deep photometric color

Probabilistic mapping between deep and wide photometric colors

In order to marginalize over deep photometric information, we must replace regions of color space with discrete categories c and $\hat{c}$.

$$p(z|\hat{c},\hat{s}) = \sum_{c} p(z|c,\hat{c},\hat{s})p(c|\hat{c},\hat{s})$$

p(z) at a given deep photometric color

Probabilistic mapping between deep and wide photometric colors

$c = (u, g, r, i, z, J, H, K)$

$\hat{c} = (r, i, z)$

$\hat{s}$ is the sample selection function

Our strategy is to leverage the deep fields in DES Y3 to improve our knowledge of the statistical color-redshift relation.

$$p(z|\hat{b},\hat{s}) = \sum_{\hat{c}\in\hat{b}} p(z|\hat{c},\hat{s})p(\hat{c}|\hat{s})$$

$$= \sum_{\hat{c}\in\hat{b}} \sum_{c} p(z|c,\hat{c},\hat{s})p(c|\hat{c},\hat{s})p(\hat{c}|\hat{s})$$

$$p(z|\hat{b},\hat{s}) \approx \sum_{\hat{c}\in\hat{b}} \sum_{c} p(z|c,\hat{b},\hat{s})p(c|\hat{c},\hat{s})p(\hat{c}|\hat{s})$$

$c = (u, g, r, i, z, J, H, K)$

$\hat{c} = (r, i, z)$

$\hat{s}$ is the sample selection function

The self-organizing map classifies galaxies of similar colors into categories called cells.

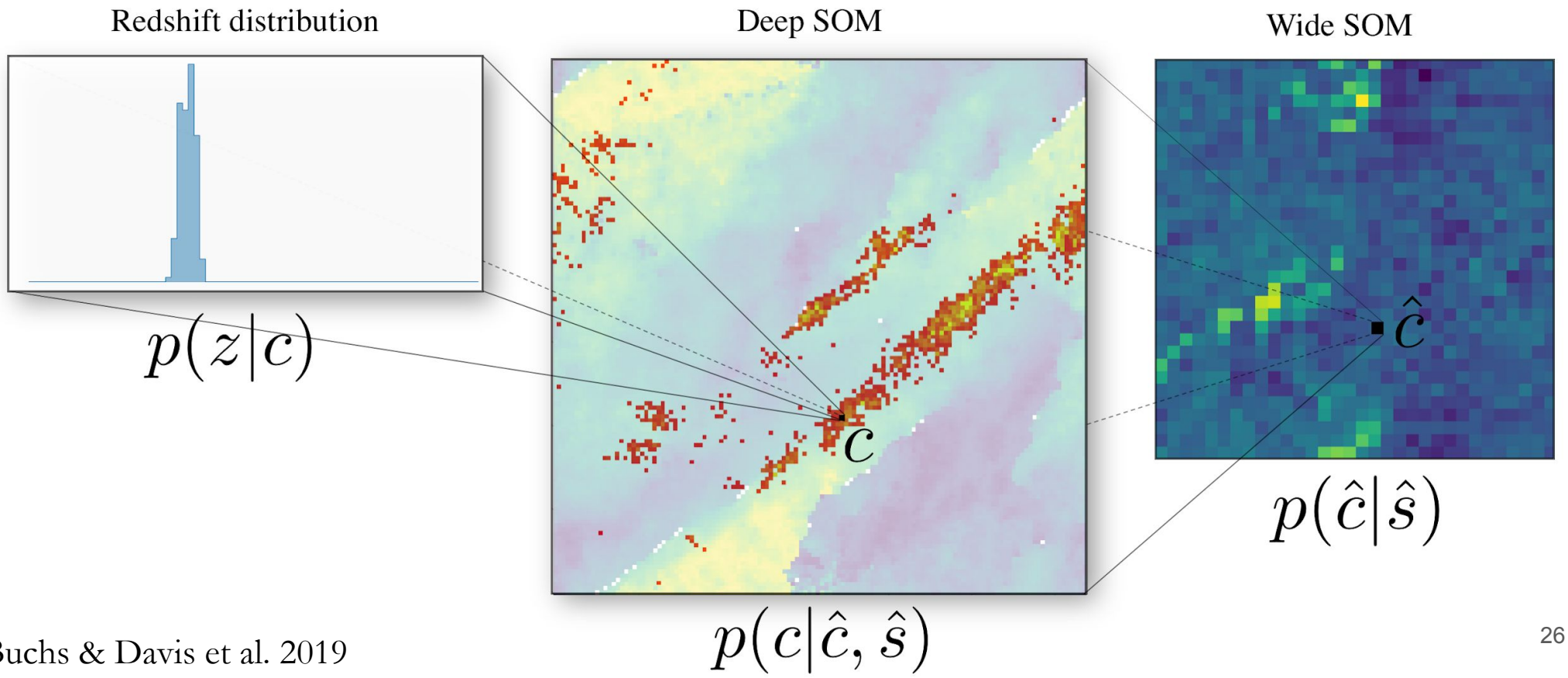

Buchs & Davis et al. 2019

$$p(z|\hat{b},\hat{s}) \approx \sum_{\hat{c}\in\hat{b}} \sum_{c} p(z|c,\hat{b},\hat{s}) p(c|\hat{c},\hat{s}) p(\hat{c}|\hat{s})$$

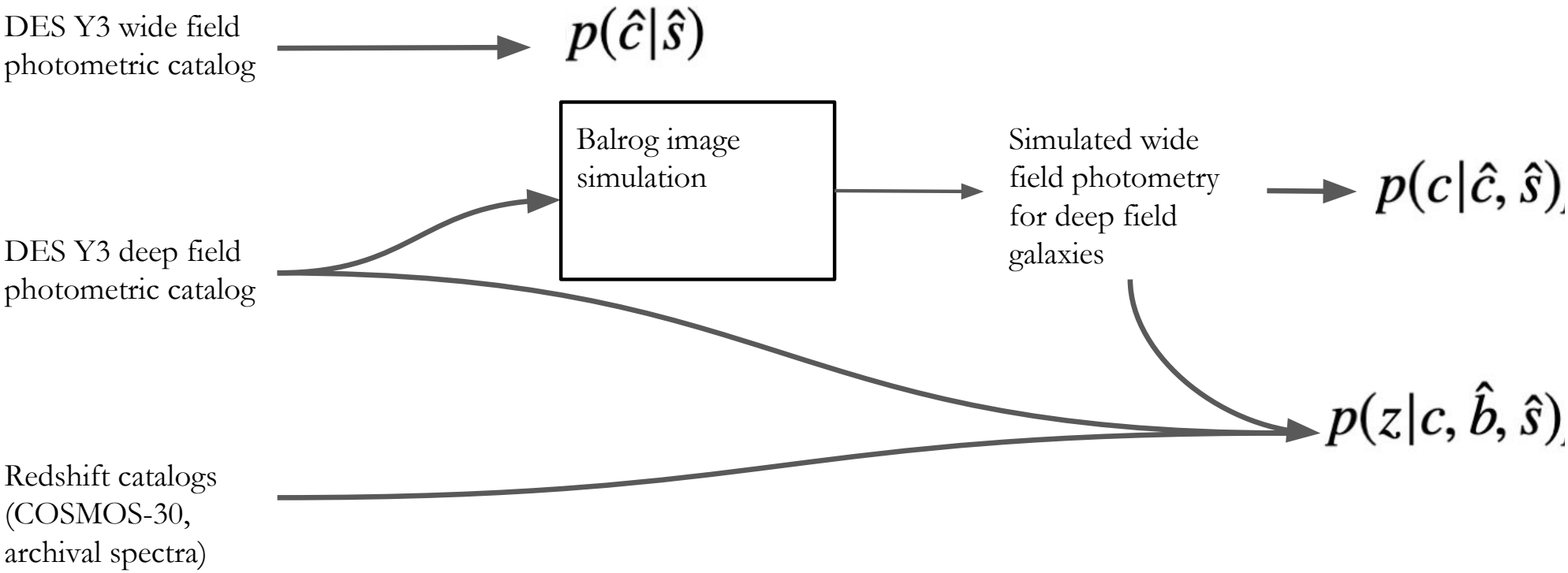

I. Motivation

II. Quantifying Projection Effects in redMaPPer Clusters

III. DES Year 3 Weak Lensing Source Galaxy Redshift Calibration

A. 3x2pt. cosmology with the Dark Energy Survey

B. SOMPZ: a novel method for weak lensing redshift calibration

C. DES Y3 Results

On average, the method recovers the true n(z) in tests on simulations.

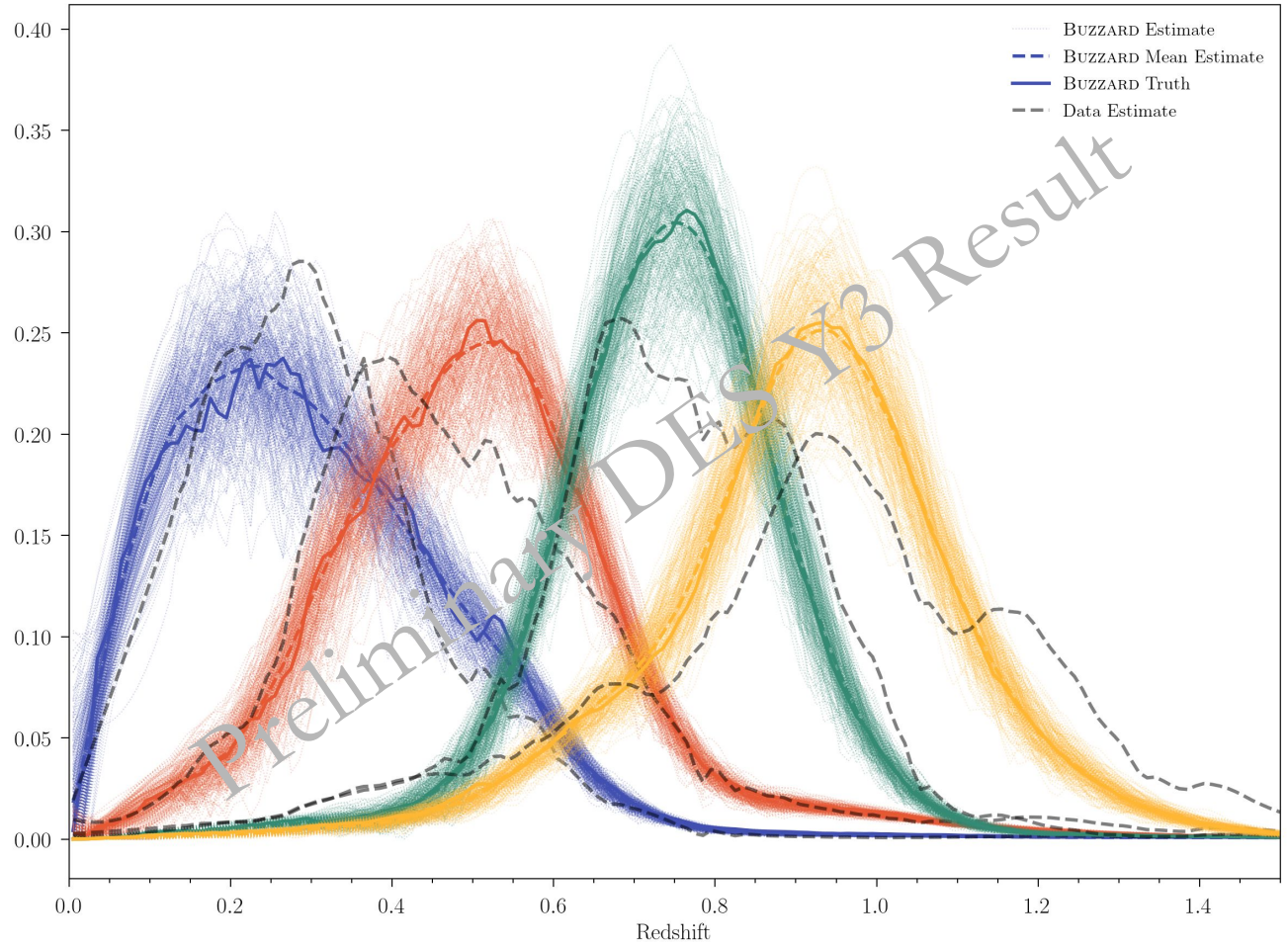

Myles & Alarcón et al. (in internal review)

We have fiducial estimates of the redshift distributions of our weak lensing source sample in four tomographic bins.

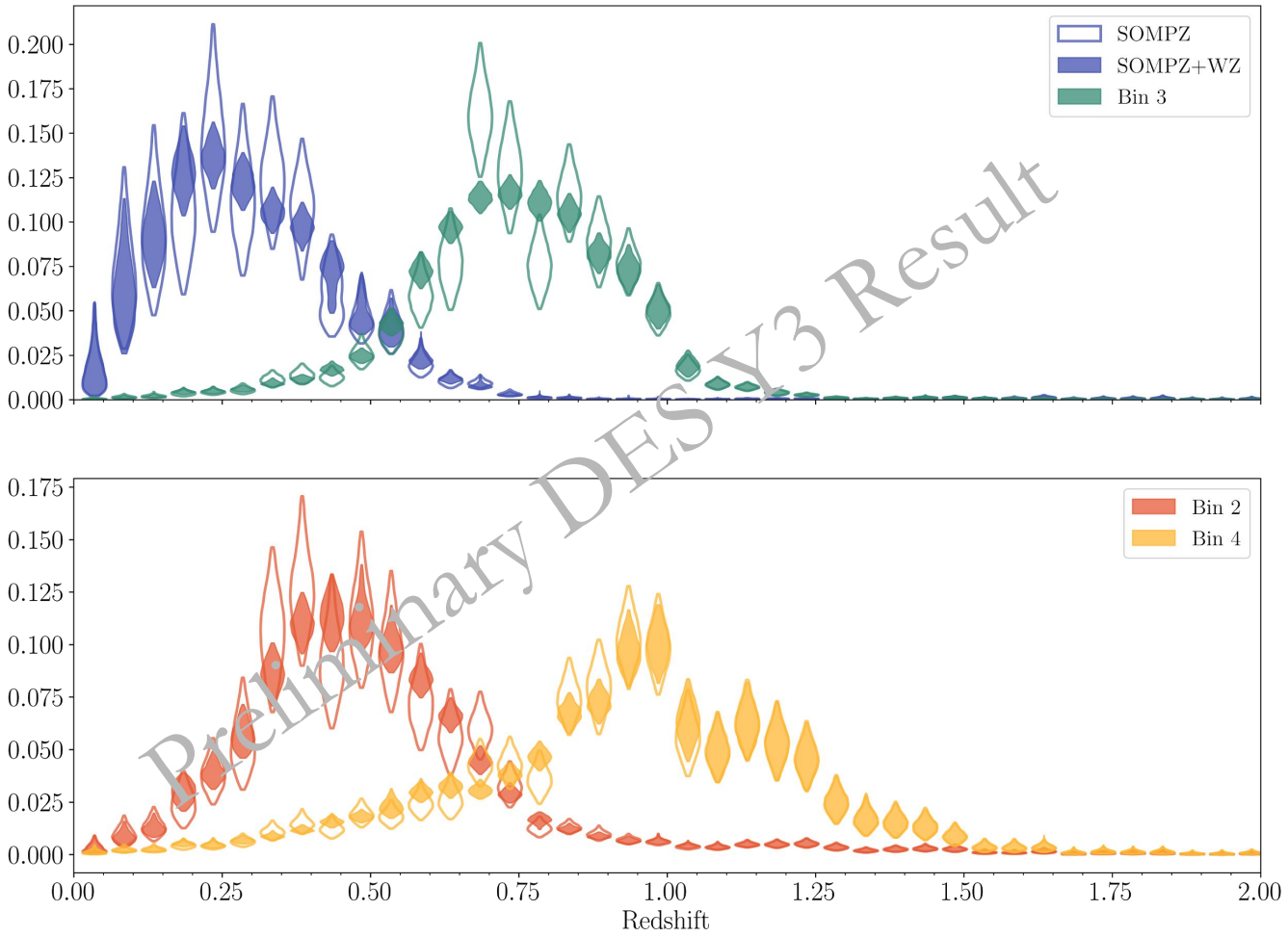

Myles & Alarcón et al. (in internal review)

Which of the following sources of uncertainty in our measurement is most important?

Shot Noise and Sample Variance in the Deep Fields	**A**
Biases in the redshift sample	**B**
Photometric calibration error in the Deep Fields	**C**
Uncertainty due to Balrog	**D**
Inherent SOMPZ Method Uncertainty	**E**

Our cosmology result will robustly account for the uncertainty in our estimate on a bin-by-bin basis.

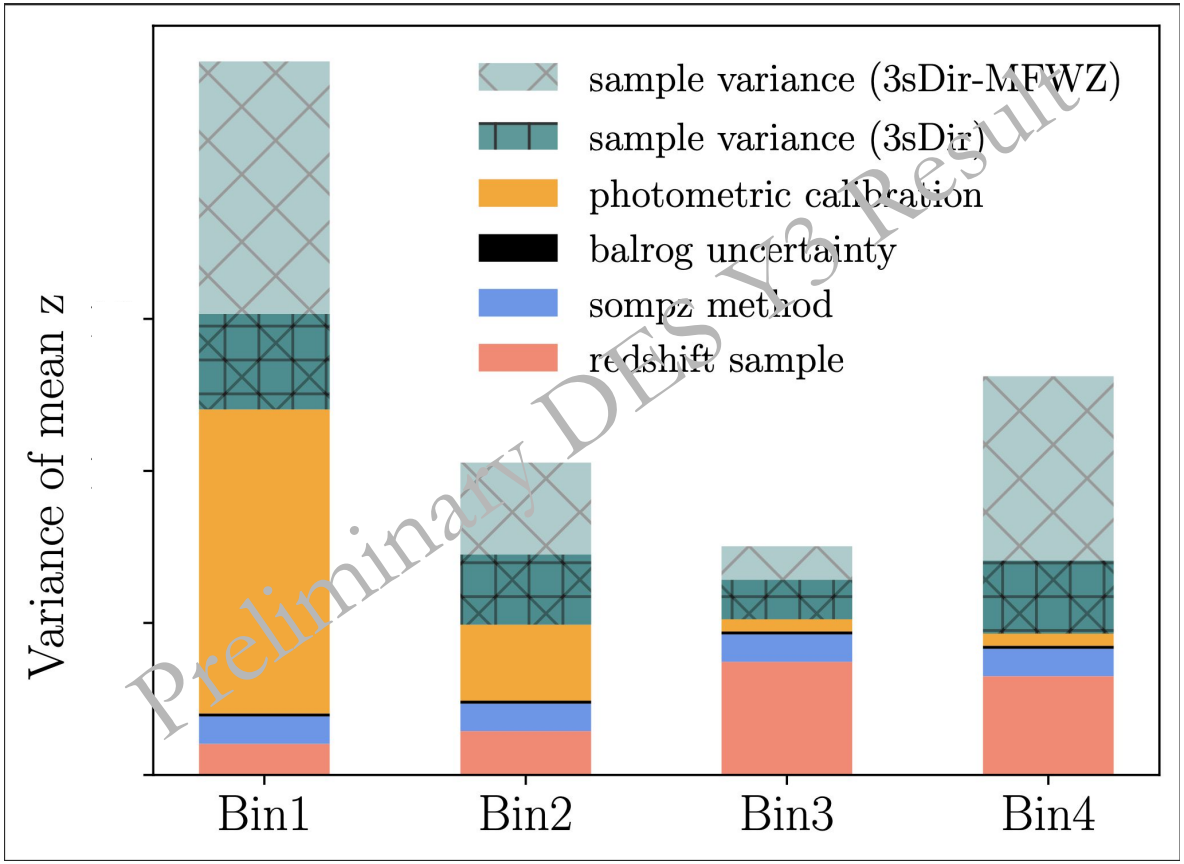

Myles & Alarcón et al. (in internal review)

Summary

1. My work aims to directly address the fundamental photo-z problem -- degeneracies in the color-redshift relation -- by leveraging spectroscopy and deep, many-band photometry.

2. Cluster Projection Effects
   - We have a direct measurement of projection effects and find greater richness dependence than previous models.
   - We need complete observations down to 0.2L* for clusters out to z~0.7
     - See DESI Spare Fiber Proposal by Golden-Marx et al.

3. Weak Lensing Redshift Calibration
   - We need to maximize the overlap of NIR and optical wide field surveys
   - We need to collect more spectra and narrow-band imaging
     - See DESI Spare Fiber Proposal to fill SOM cells by Gruen, Amon, McCullough et al.
   - We need to improve the photometric calibration of our deep fields

Credits

Projection Effects Team: Steve Allen, Rodrigo Carrasco, Matteo Costanzi, Joe DeRose, Daniel Gruen, Tesla Jeltema, Anthony Kremin, Rich Kron, Adam Mantz, Glenn Morris, Eduardo Rozo, Eli Rykoff, Chun Hao To, Risa Wechsler

SOMPZ Team: Àlex Alarcón, Gary Bernstein, Andresa Campos, Ami Choi, Alex Amon, Juan Pablo Cordero, Joe DeRose, Scott Dodelson, Spencer Everett, Marco Gatti, Giulia Giannini, Daniel Gruen, Ian Harrison, Will Hartley, Huan Lin, Jamie McCullough, Justin Myles, Aaron Roodman, Carles Sánchez, Michael Troxel, Boyan Yin, et al.

Deep Fields Team: Alex Amon, Gary Bernstein, Ami Choi, Katie Eckert, Daniel Gruen, Ian Harrison, Will Hartley, Robert Gruendl, Mike Jarvis, Nacho Sevilla, Erin Sheldon, et al.

Balrog Team: Spencer Everett, Eric Huff, Nikolay Kuropatkin, Brian Yanny, et al.

Extra Slides

Projection effects are a strong function of richness.

$$b_{\lambda,j} \equiv \frac{\sum_{m \in j} p_{\rm phot} - \sum_{m \in j} p_{\rm spec}\, p_{\rm red}\, p_{\rm free} \theta_r \theta_i}{\sum_{m \in j} p_{\rm phot}}$$

$$= \frac{\sum \lambda^{L \geq 0.55\, L_\star} - \sum {\lambda_{\rm spec}}^{L \geq 0.55\, L_\star}}{\sum \lambda^{L \geq 0.55\, L_\star}}.$$

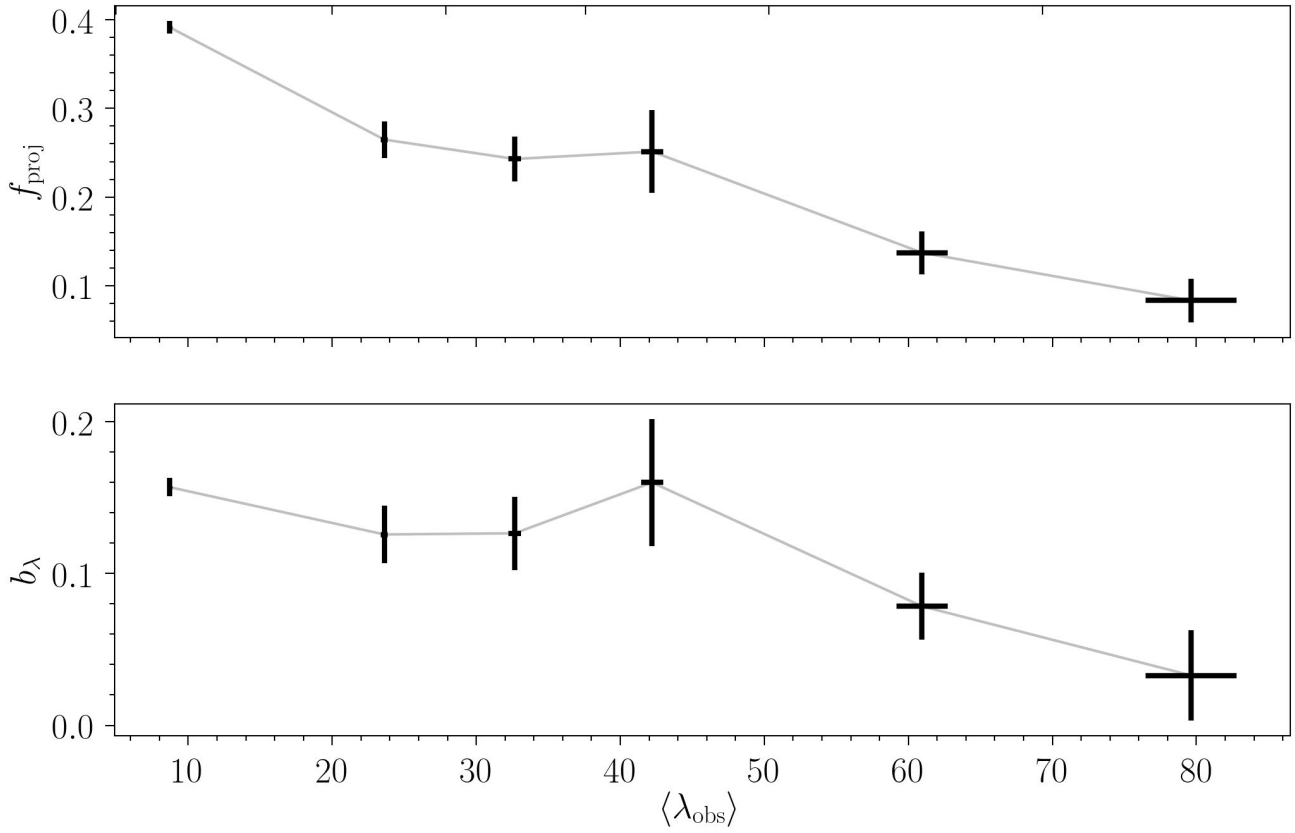

Myles et al. 2020 (arXiv: 2011.07070)

As light passes massive structures, it is bent due to gravity. This effect shifts, magnifies, and shears the galaxy image.

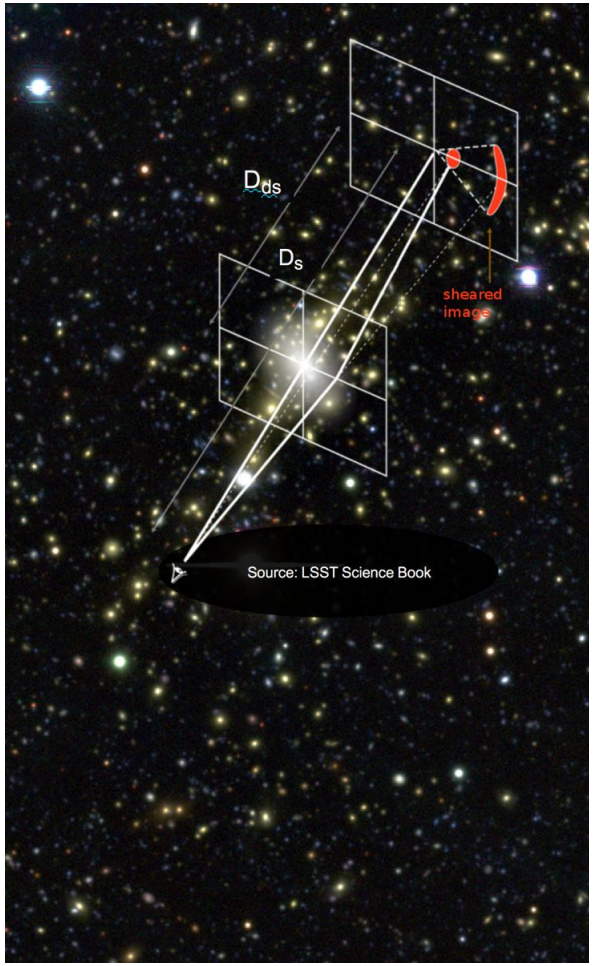

As light passes massive structures, it is bent due to gravity. This effect shifts, magnifies, and shears the galaxy image.

$$\gamma_t(\theta) = \langle\kappa(\theta')\rangle_{\theta'<\theta} - \kappa(\theta)$$

$$\kappa = \Sigma / \left[\frac{c^2}{4\pi G}\frac{D_\mathrm{s}}{D_\mathrm{d} D_\mathrm{ds}}\right]$$

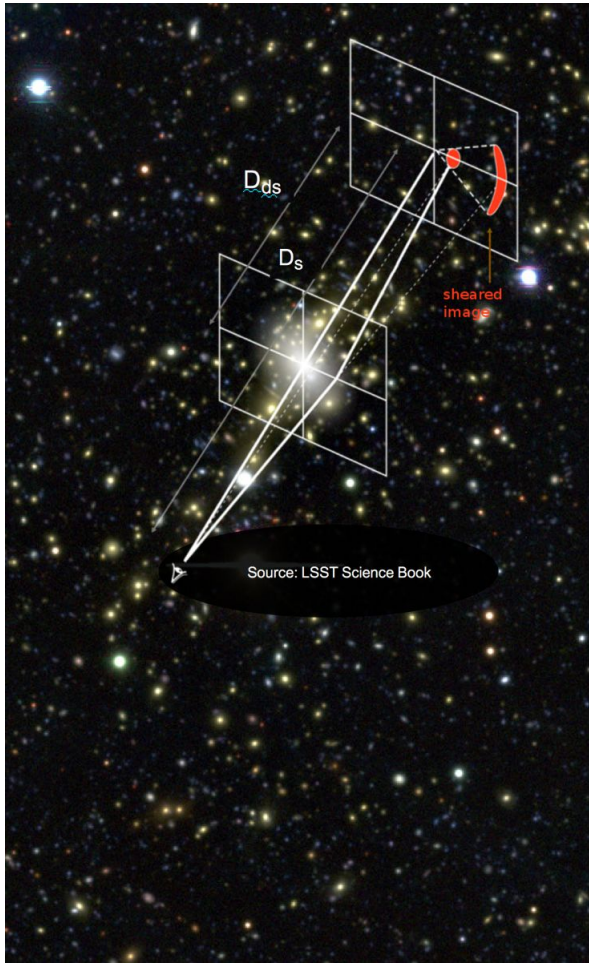

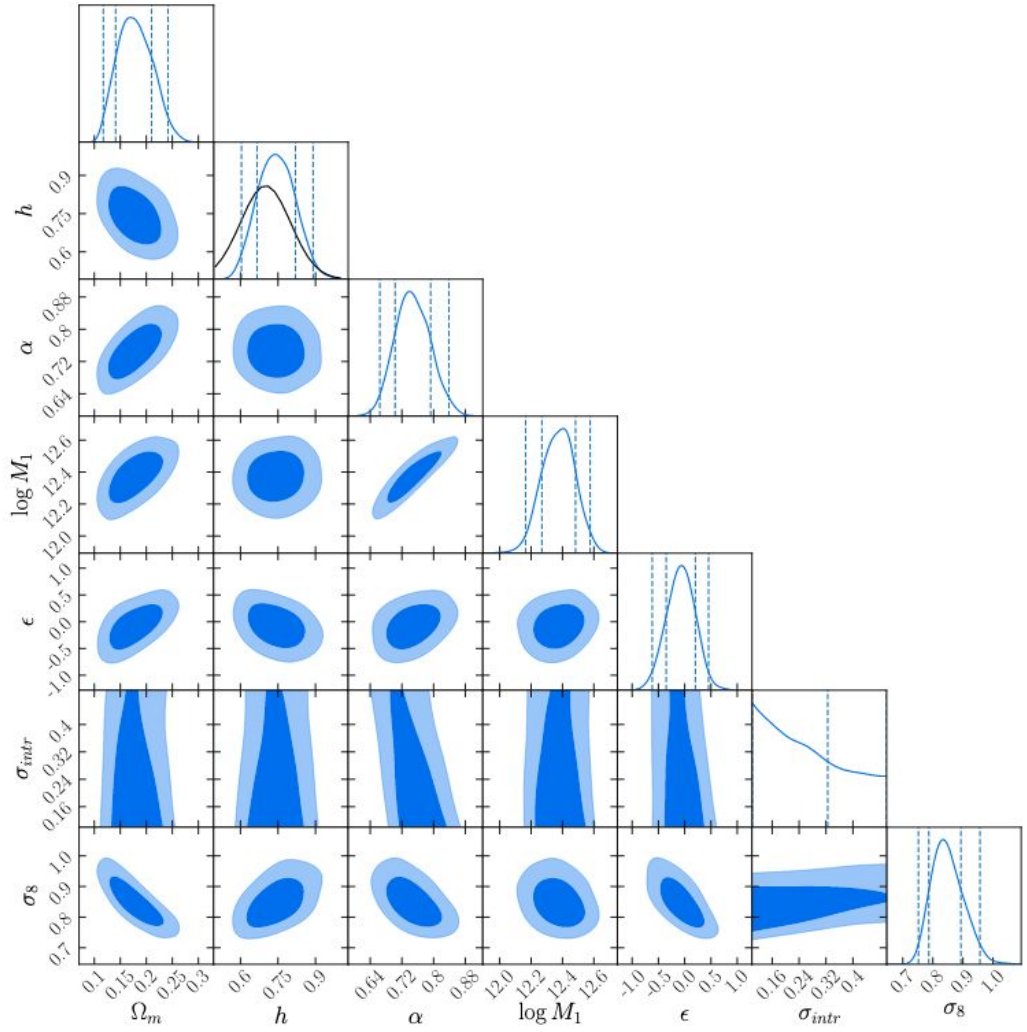

FIG. 4. Marginalized posterior distributions of the fitted parameters. The $2D$ contours correspond to the 68% and 95% confidence levels of the marginalized posterior distribution. The dashed lines on the diagonal plots correspond respectively to the 2.5th, 16th, 84th and 97.5th percentile of the 1-d posterior distributions. The black line in the 1-d posterior plot of h corresponds to the Gaussian prior adopted in the analysis. The description of the model parameters along with their posteriors are listed in Table III. Only parameters that are not prior dominated are shown in the plot.

DES Collaboration et al. 2020

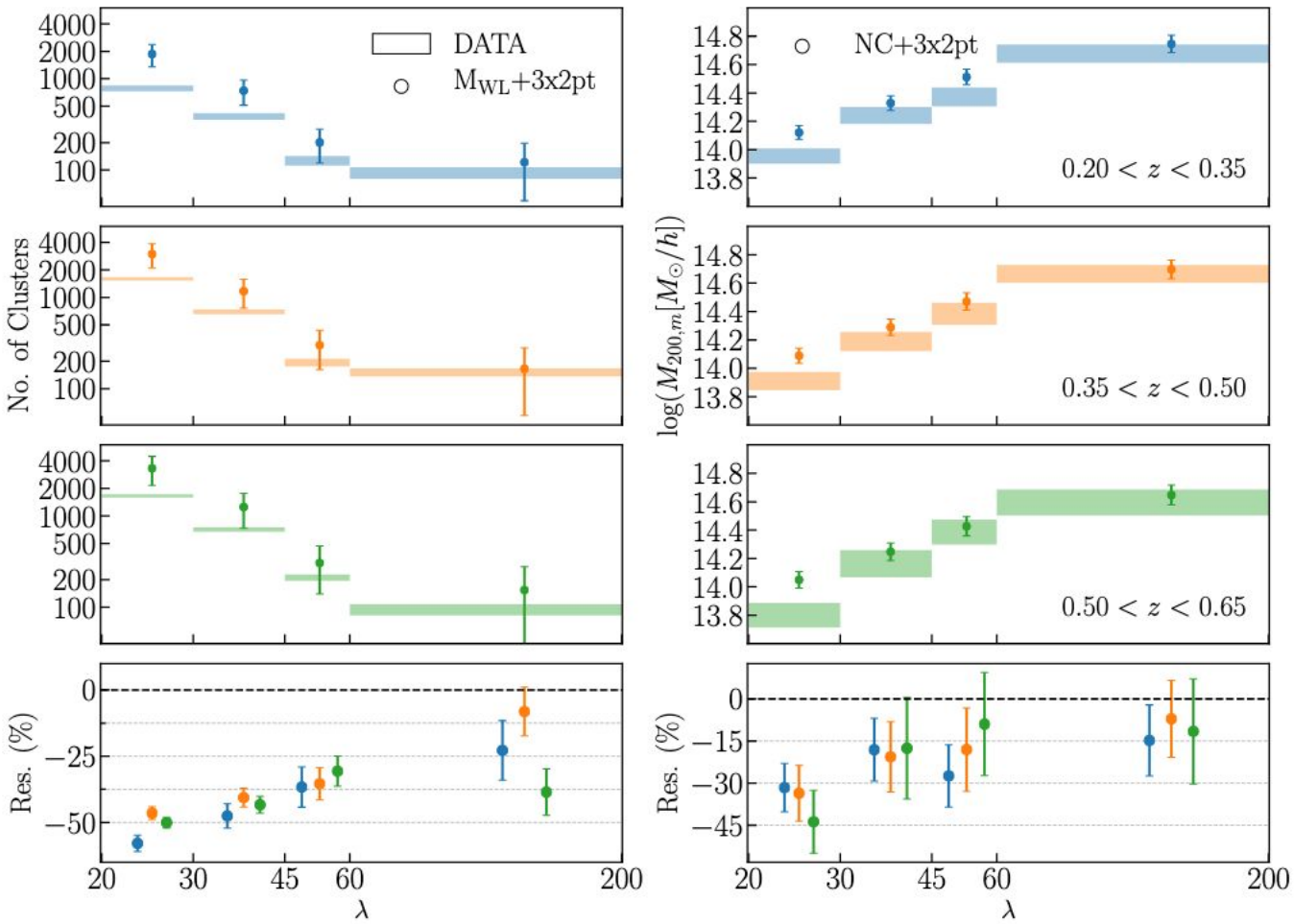

FIG. 11. Comparison of the observed data vectors (*shaded areas*) with the number counts predicted from the combination of weak-lensing mass estimates and DES Y1 3x2pt cosmology (*left* panel), and mean masses predicted from the combination of Y1 number counts data and DES Y1 3x2pt cosmological priors (*right*). The y extent of the *shaded areas* correspond to the error associated with the data. The error bars on the predicted number counts and mean masses represent one standard deviation of the distribution derived sampling the corresponding MCMC chain. The lower panel shows the percent residual of the predictions to the data vectors, where the error bars refer to data vector uncertainties.

DES Collaboration et al. 2020

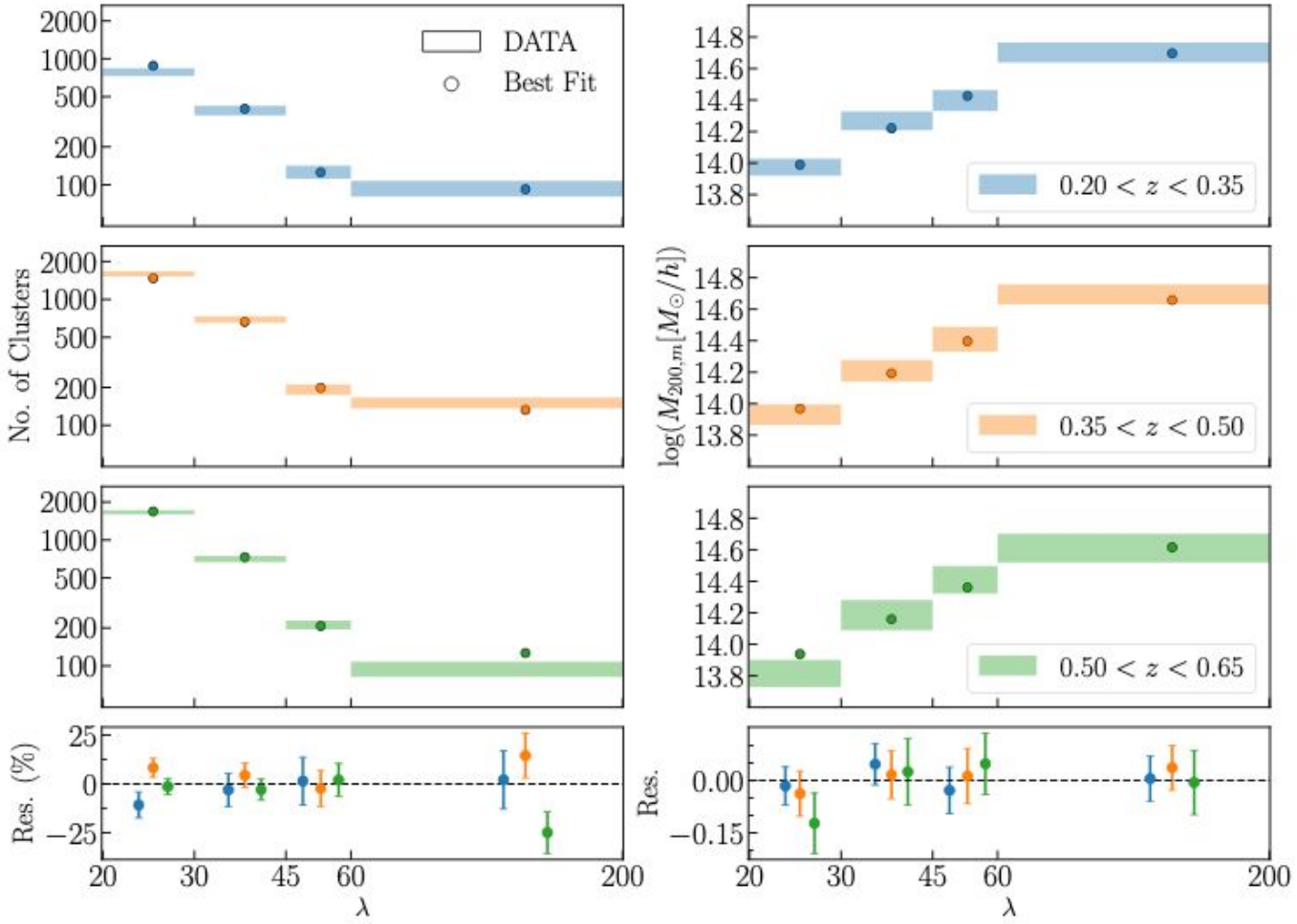

FIG. 2. Observed (*shaded areas*) and best-fit model (*dots*) for the cluster number counts (*left*) and mean cluster masses (*right*) as a function of richness for each of our three redshift bins. The y extent of the data boxes is given by the square root of the diagonal terms of the covariance matrix. The bottom panel shows the residual between the data and our best-fit model. All points have been slightly displaced along the richness axis to avoid overcrowding.

DES Collaboration et al. 2020

The parameters of the projection component are consistent across bins.

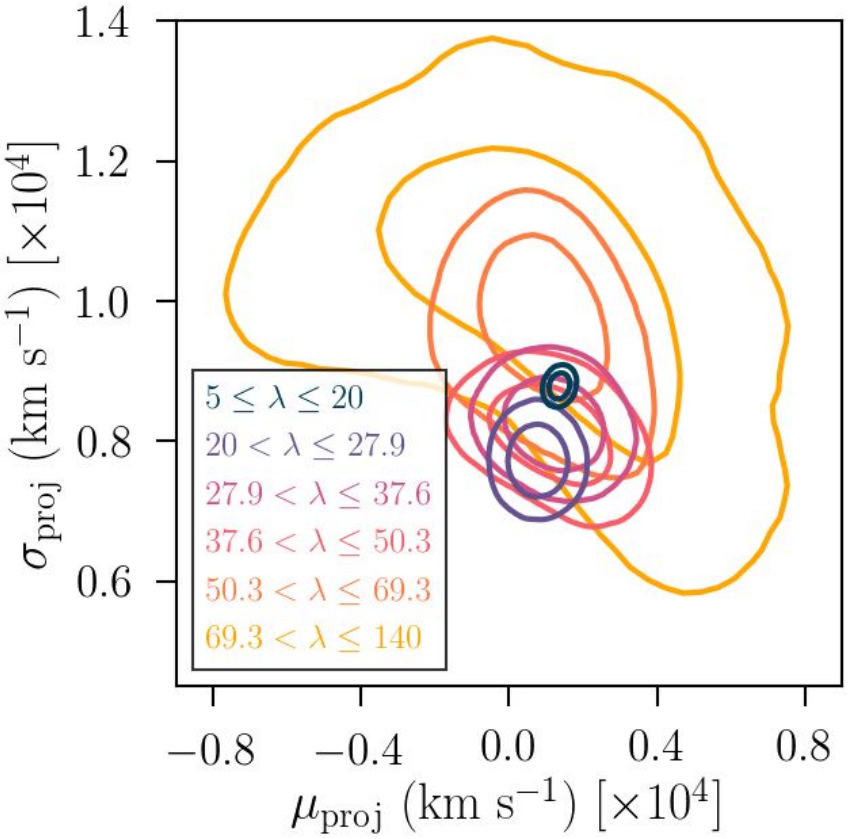

Myles *et al.* 2020 (arXiv: 2011.07070)

The cluster component is consistent with zero mean.

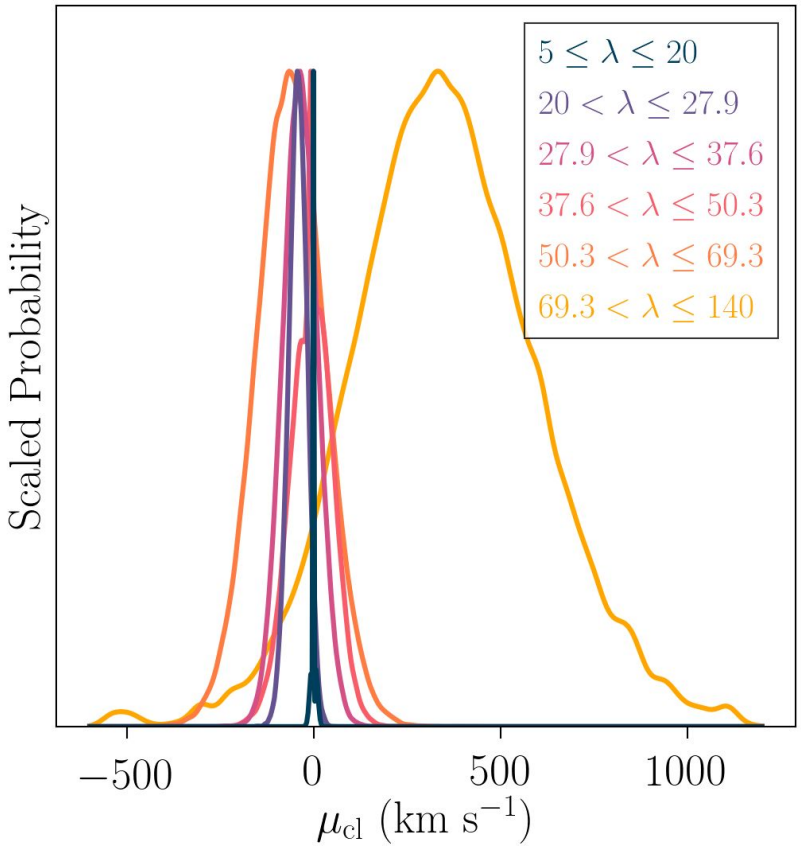

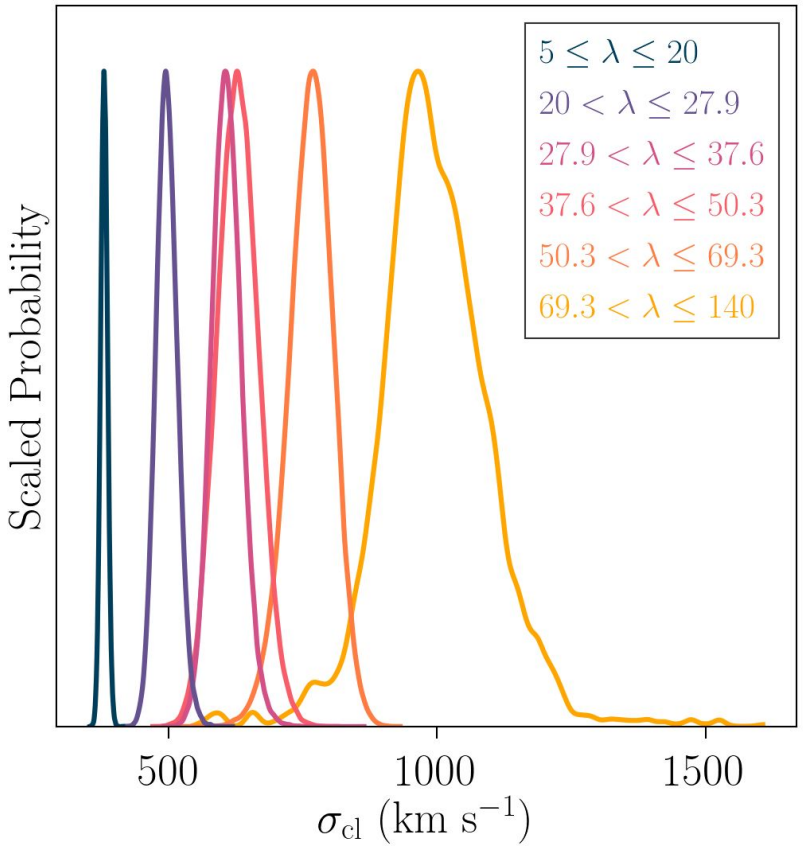

Myles *et al.* 2020 (arXiv: 2011.07070)

Cluster photo-zs are too noisy to do our measurement.

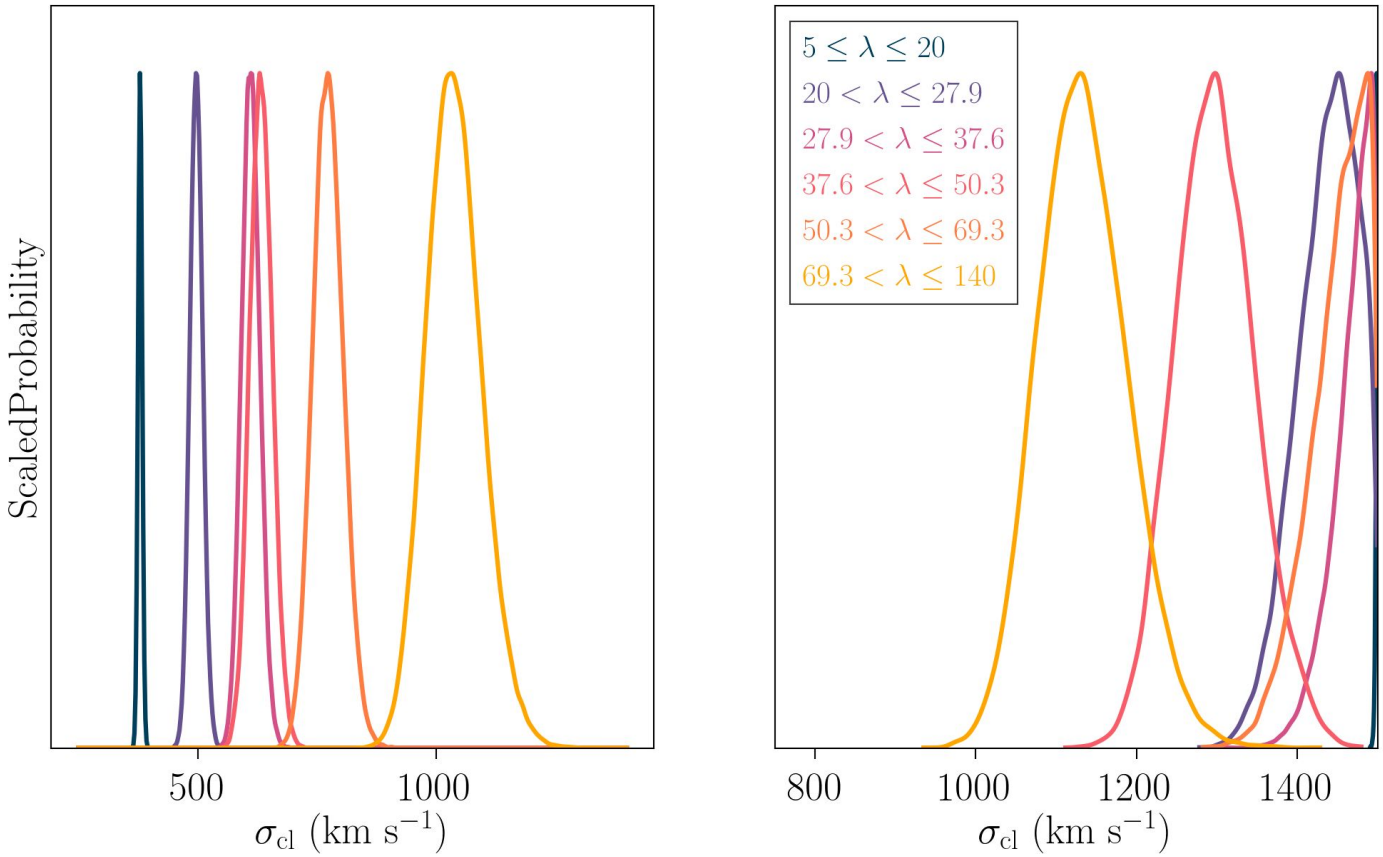

Myles *et al.* 2020 (arXiv: 2011.07070)

Testing a cosmological model with cosmic shear depends on a statistical ensemble of two basic measurements: galaxy shapes and redshifts.

$$\hat{\xi}^{ij}_{\pm}(\theta) = \frac{1}{2\pi} \int d\ell \ell J_{0/4}(\theta\ell) P^{ij}_{\kappa}(\ell)$$

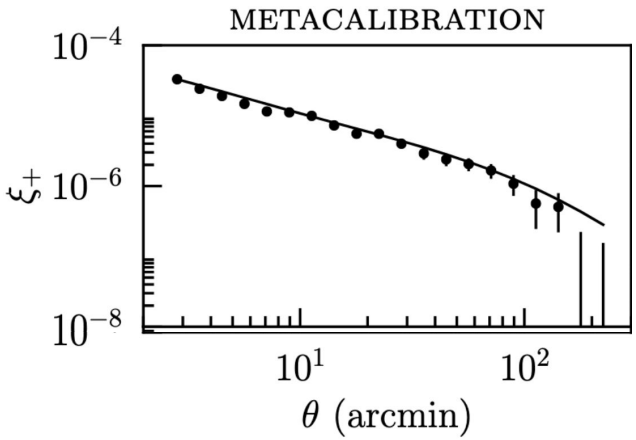

Troxel *et al.* 2018

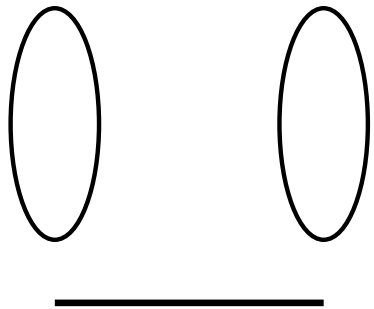

Θ

The similar alignment of these two galaxies leads to a positive contribution to ξ^+

A modern cosmological analysis necessarily depends on using numerous independent constraints and sophisticated sampling procedures over relevant uncertainties to verify the robustness of the overall measurement.

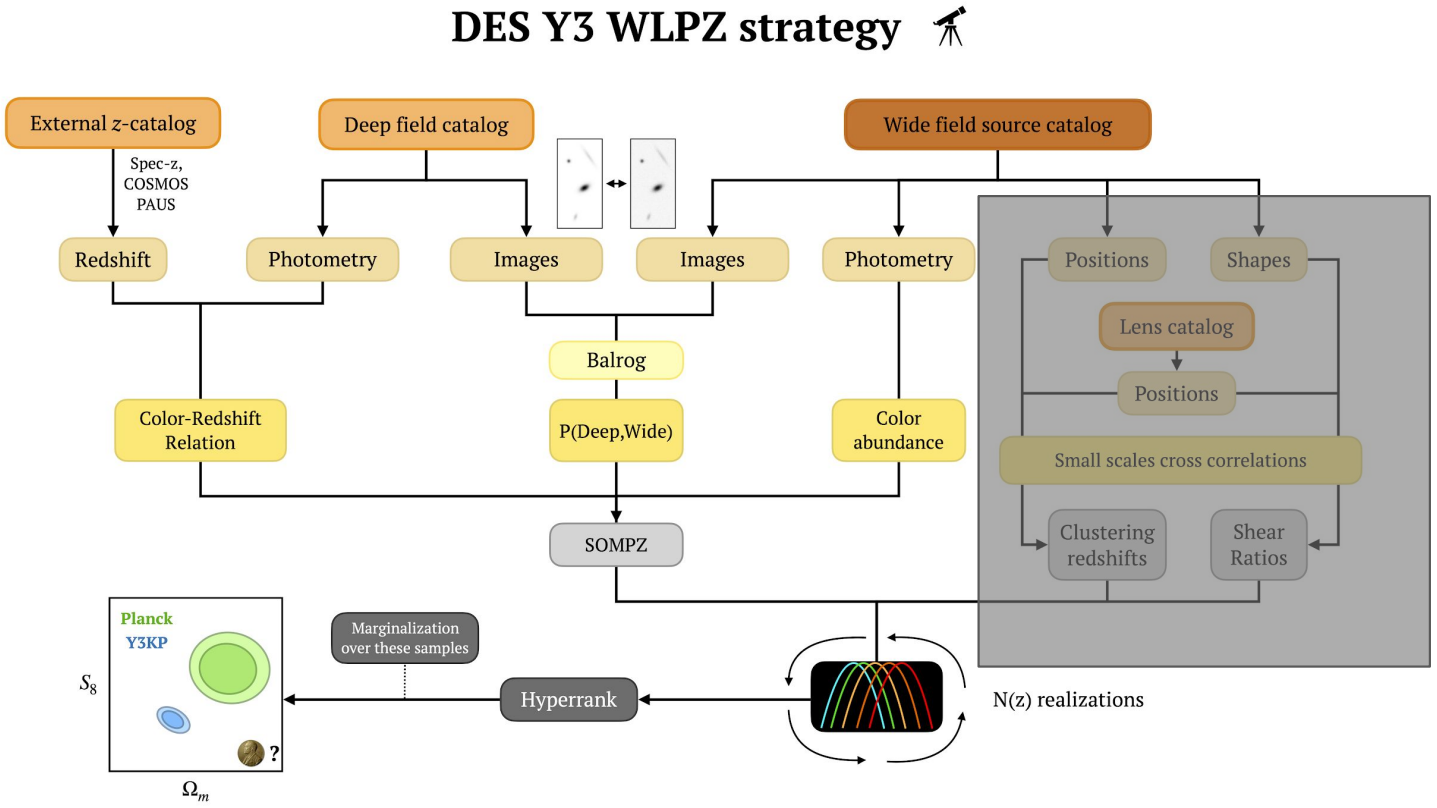

Credit: Àlex Alarcón and Judit Prat

The self-organizing map learns to smoothly cover color space, which facilitates interpolation of cells for which we have less than average counts.

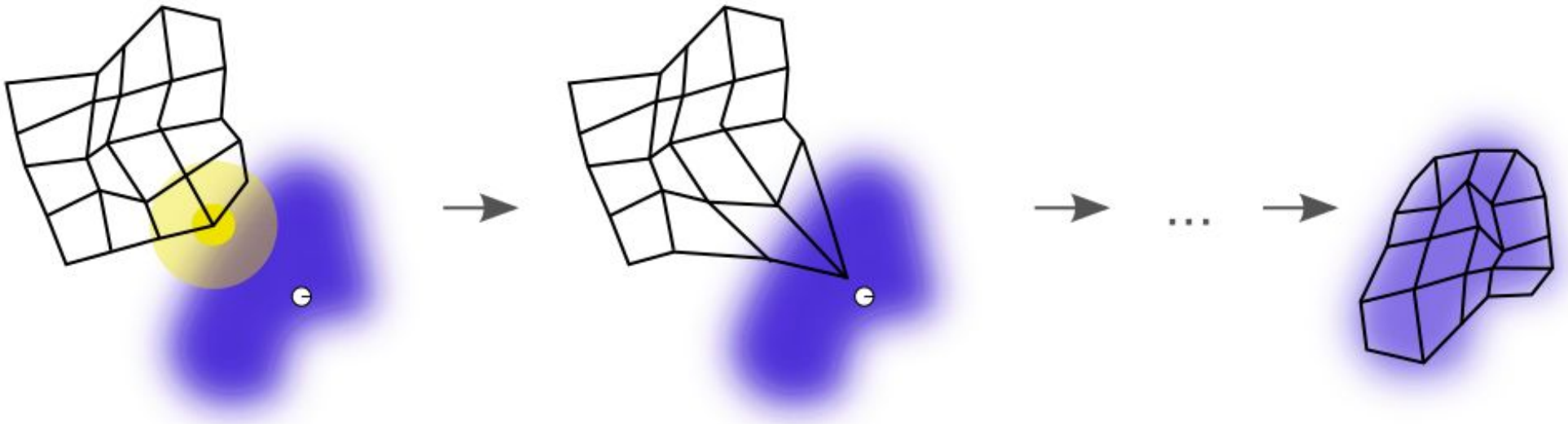

The self-organizing map groups together galaxies of similar colors in cells.

Training Input i: 

step i

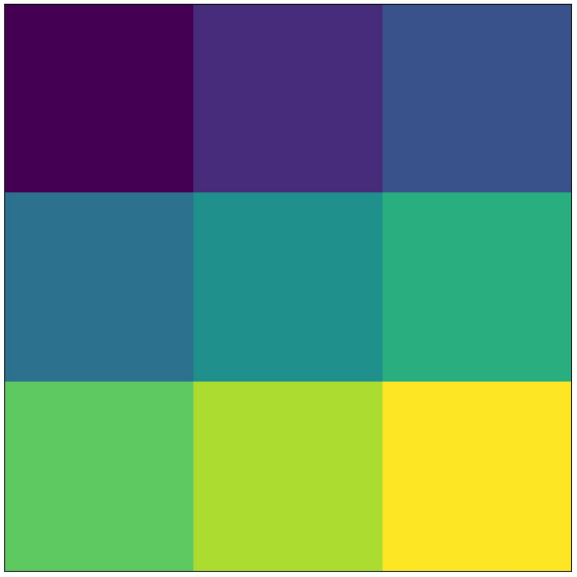

step i+1

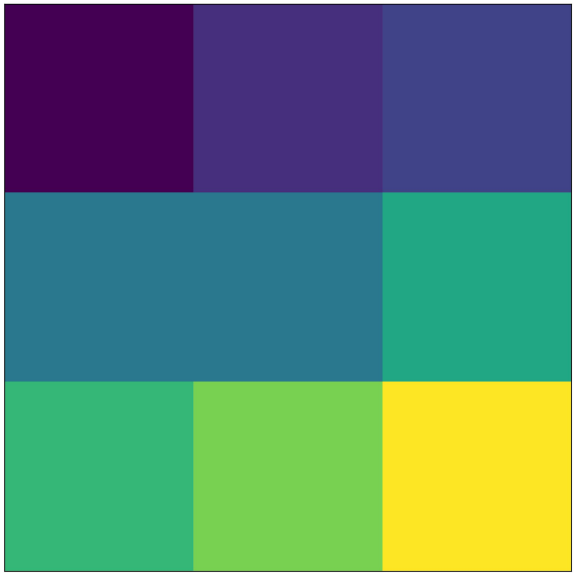

We can leverage overlap of DES deep fields with archival NIR data

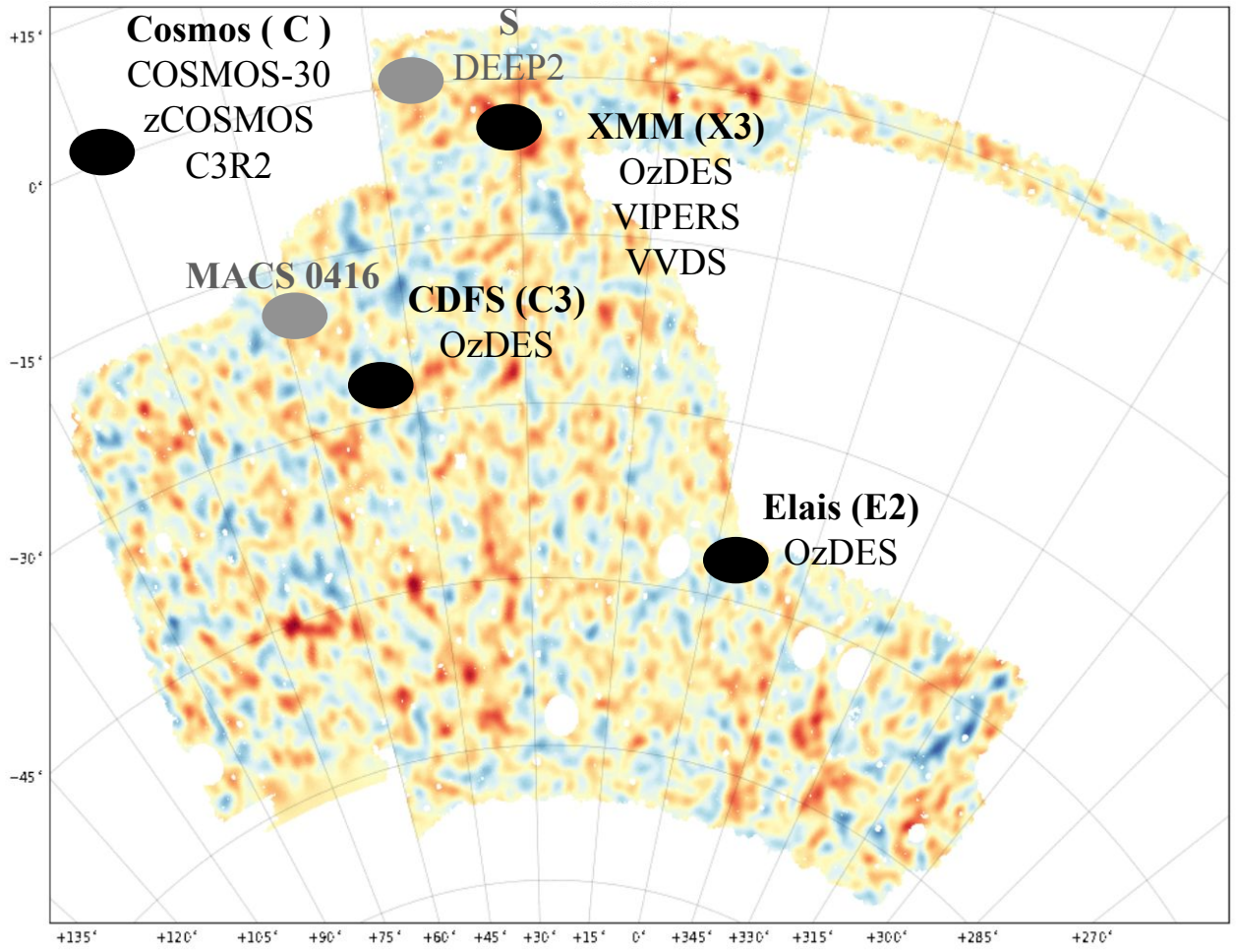

Figure Credit: Alex Amon and DES Deep Fields Team

The Deep Fields : deep DECam photometry + NIR

Field	COSMOS (C)	CDFS (C3)	XMM (X3)	Elais (E2)
NIR data	Ultravista	VIDEO	VIDEO	VIDEO
bands	*ugrizY YJHKs*	*ugrizY JHKs*	*ugrizY YJHKs*	*ugriz YJHKs*
Exposure time (sec.)	200x90	200x90	200x90	80x90
Overlap area (sq. deg.)	1.38	(1.94)	3.29	3.32

Figure Credit: Alex Amon, Will Hartley, Deep Fields Team

Total: 7.99 sq. deg. (9.93 no Y)

Slide omitted

Slide omitted

Our cosmology result will robustly account for the uncertainty in our estimate due to the **photometric calibration error** of the deep fields.

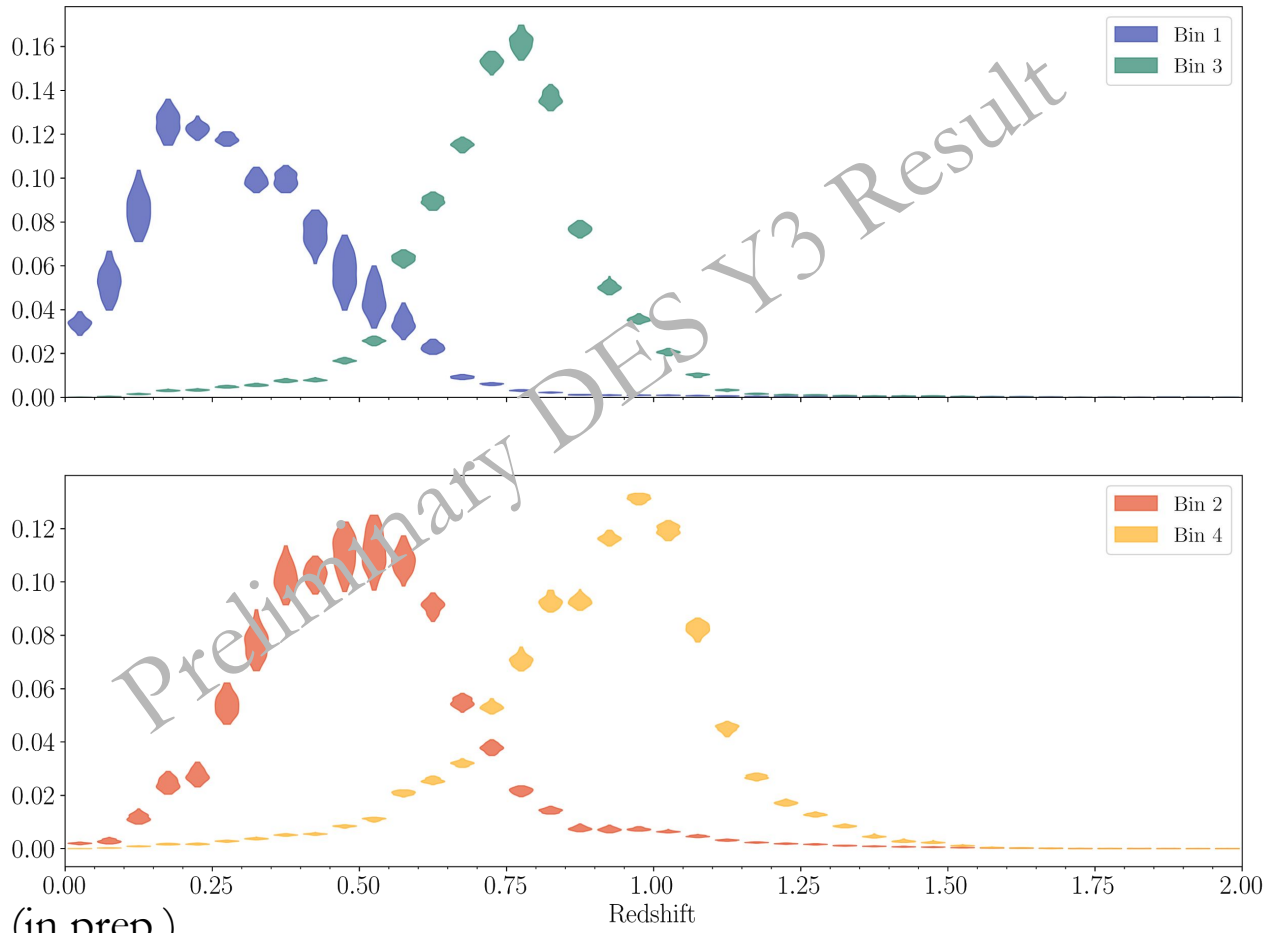

Myles & Alarcón *et al.* (in prep.)

Construction of bins is done by assigning each galaxy in our Balrog sample to a tomographic bin according to some arbitrary bin edges such that each bin have a similar number of galaxies, and assigning each wide som cell to the bin to which a plurality of its constituent Balrog galaxies are assigned.

The analysis on Buzzard (Buchs et al. 2018) suggests we are limited by deep fields.

- The scatter in the bias of the mean inferred redshift is dominated by limited deep fields, not limited redshift samples. This motivates follow-up observations overlapping with existing infrared surveys.
- The pheno-z method can reduce cosmic variance significantly.